Journal of Hydrology: Regional Studies 56 (2024) 102039

Contents lists available at ScienceDirect

Journal of Hydrology: Regional Studies

journal homepage: www.elsevier.com/locate/ejrh

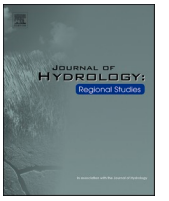

Disentangling hydrodynamic drivers of the Southern Venice (Italy) coastal aquifer via frequency decomposition analysis: Insights, challenges, and limitations

Mattia Gaiolini [a], Fabrizio Rama [b], Micòl Mastrocicco [c], Marta Cosma [d], Sandra Donnici [d], Luigi Tosi [d,*], Nicolò Colombani [a,*]

[a] Department of Materials, Environmental Sciences and Urban Planning, Polytechnic University of Marche, Via Brecce Bianche 12, Ancona 60131, Italy
[b] Syngenta Jealott's Hill International Research Centre, Environmental Safety, Warfield, Bracknell RG426EY, United Kingdom
[c] Department of Environmental, Biological and Pharmaceutical Sciences and Technologies, Campania University "Luigi Vanvitelli", Via Vivaldi 43, Caserta 81100, Italy
[d] Institute of Geosciences and Earth Resources, National Research Council, Corso Stati Uniti 4, 35127 Padova, Italy

ARTICLE INFO

Keywords:
U-Tide
Surface water level
Groundwater level
Salinity
Interconnection
Leakage

ABSTRACT

Study region: Shallow coastal aquifer located in the southern part of the Venice lagoon (Italy).
Study focus: This study aims to improve the understanding of coastal aquifers' hydrodynamics by implementing systematic time-series analyses of data. A collection of non-intrinsically consistent time series from hydrological (surface water and groundwater) and meteo-mareographic monitoring networks was obtained from different institutions. Each signal was broken down through a frequency decomposition analysis, isolating the main driving forces to focus on phenomena that occur at different time and spatial scales.
New hydrological insights for the region: Results highlighted that the aquifer is highly connected with the Venice lagoon, with a clear fluctuation of piezometric heads induced by tidal major constituents, decreasing landward. Besides, the effects exerted by reclamation canals and pumping stations were also determined and found to increase landward. Despite the relatively simple behaviour of piezometric heads, the groundwater salinity is influenced by additional local factors, like probe depth, wells' screen length, and vertical salinity distribution along the aquifer. These findings suggested how to make use of limited and sparse data to enhance the conceptual model of coastal aquifer hydrodynamics, while highlighting the limitations of existing monitoring networks. This outcome justified the need for an intrinsically-consistent network of dedicated multi-level samplers to avoid intra-borehole mixing and reliably characterize the groundwater salinity distribution.

1. Introduction

One of the most important and usually overlooked resources that support life on our planet is groundwater. This valuable water reserve is hosted in the void within the subsurface and offers many services to humankind and living species. It provides freshwater

* Corresponding authors.
E-mail addresses: luigi.tosi@igg.cnr.it (L. Tosi), n.colombani@univpm.it (N. Colombani).

https://doi.org/10.1016/j.ejrh.2024.102039
Received 23 June 2024; Received in revised form 15 September 2024; Accepted 17 October 2024
Available online 31 October 2024

(Baggio et al., 2021; Foster et al., 2013), maintains ecosystem services (Nevill et al., 2010; Saito et al., 2021), and supports economic activities, such as worldwide agriculture and food production (Foster and Garduño, 2013; Malki et al., 2017), which rely almost completely on groundwater availability, especially in coastal regions that are the most affected by the ongoing climate change (Amanambu et al., 2020; Green et al., 2011).

In the last decades, the demand for groundwater has been exacerbated by several environmental and anthropogenic factors that created a spectrum of challenges endangering the sustainability of these vital but fragile reservoirs (Burri et al., 2019; Han et al., 2017). Extensive over-extraction (Khorrami and Malekmohammadi, 2021) and seawater intrusion (Mastrocicco and Colombani, 2021) represent critical challenges for the resilience of groundwater resources. Understanding the hydrodynamics of groundwater systems is pivotal to effectively address these issues (Naganna et al., 2017; Rojas et al., 2010), holistically and in the long term. The first step is the delineation of a clear and robust subsurface conceptual model that disentangles groundwater flow dynamics, by providing a systematic and internally coherent overview of system boundaries, properties, and mechanisms within the domain (Enemark et al., 2019). Observation and monitoring data are deployed in such an effort to set constraints and to limit the variability of the natural system in the model, starting usually from the best and most abundant information available.

In that framework, research approaches in coastal aquifers often use filtering of the groundwater head data as a starting point, to study tidal and non-tidal influences on groundwater heads separately (Sánchez-Úbeda et al., 2016). Tide studies make use of the decomposition and adjustment of periodic and aperiodic components to reconstruct raw signals and predict their evolution over time (Brown et al., 2012; Codiga, 2011; Erol, 2011). Classical Harmonic Analysis (CHA) and Continuous Wavelet Transforms (CWT) are the main methodologies for processing tidal data (Labat, 2005). In the last few years, several codes were developed in MATLAB based on CHA. Most of them were summarized into the T_TIDE package (Pawlowicz et al., 2002). Subsequent evolutions include U_TIDE, which was developed to unify tidal analyses and the prediction framework (Codiga, 2011), and NS_TIDE (Matte et al., 2013). Consequently, hydrogeological studies have tried to assess tidal influences on groundwater using such tools, assuming that a Dirichlet (or first-type) condition is the main boundary of the subsurface system, and thereby, the transient variation of the downgradient receptor elevation is the main driver of the hydrodynamic of shallow coastal aquifers very close to the shore. Sánchez-Úbeda et al. (2016) used both CHA and CWT to filter groundwater head time series from the tide-induced oscillation. Schweizer et al. (2021) systematically tested the discrete Fourier transform and harmonic least squares methodology to extract harmonic component properties, suggesting the latter as a more robust approach. Others works, such as Rama et al. (2018) and Zhang (2021), used U_TIDE to assess periodic tide-induced water table oscillation and estimate other important aquifer parameters to be used in numerical modelling. However, only few works highlighted the importance of considering also tidal effects when studying phenomena such as seawater intrusion. Heiss and Michael (2014) observed that water table fluctuations driven by tidal amplitude and stage resulted in highly variable groundwater salinity at the land/sea interface, while Lovrinović et al. (2023) used discrete Fourier transform methodology to infer seawater intrusion responses to tidal oscillation and other natural forcings in a shallow coastal aquifer facing the Adriatic Sea. Most of the available studies miss a comprehensive picture of the natural drivers, expressed as a combination of periodic and aperiodic stresses, and how they affect the specific system over time. This paper aims to show how an analysis of time series, both in the time and frequency domain, can be deployed to widen and improve the conceptual model of a coastal aquifer, by systematically isolating the main driving forces (i.e. tides, pumping stations, river stages, flooding, and recharge), and by describing their evolution and effect over time.

The northern part of the Adriatic coastal plain near the Venice lagoon (Italy) is an important and fragile environment, impacted by land subsidence, seasonally recurring floodings, and strong seawater intrusion (Carbognin et al., 2006; Pousa et al., 2007; Teatini et al., 2005; Tosi et al., 2009b). Freshwater in the subsurface is very limited, emphasizing the urgent need to protect these vital water resources for the sustainability of ecosystems and human well-being. At the same time, the plain is an economic lung for the region with vital agricultural and economic activities that are threatened by the unstable balance of natural elements in the area. For this reason, a monitoring network has been installed to “predict” the major unexpected shifts in the conditions and the subsequent impacts on human activities.

It is worth remembering though, that the major limits of the standard monitoring network for groundwater salinization are often due to (i) large areas to be monitored (Delsman, 2015; Shi and Jiao, 2014), and (ii) a lack of dedicated depth-specific monitoring wells, except for well-documented cases (De Louw, et al., 2010; Heiss and Michael, 2014; Luo et al., 2017; Mastrocicco et al., 2012). Recent analyses of the site suggested among others: (i) a hydraulic connection among canals, pumping stations, the Venice lagoon, and the coastal aquifer (Lovrinović et al., 2021), (ii) a fluctuating fresh-/salt-water interface within the fully screened monitoring wells, closely related to the subsurface architecture (Cavallina et al., 2022), and (iii) a presence of hypersaline paleo-seawater layers, which further complicate the conceptual model of groundwater salinization (Alessandrino et al., 2023). By interacting with and expanding those insights, the present work had also the goal of providing the very first comprehensive conceptual model of the study area, which highlights the effect of the main drivers on the hydrodynamic of the shallow aquifer, identifies the flaws of the current monitoring network to address the drivers of the system, and extrapolates general learnings and knowledge gaps to work on different study areas.

2. Material and methods

2.1. The study area

The study site is located in the northern Adriatic coastal plain (Italy) approximately 500 m south of the Venice lagoon (Fig. 1). It features low-lying agricultural lands resulting from several centuries of morphological and hydrological changes, e.g. river diversion (Bondesan and Furlanetto, 2012; Parrinello et al., 2021), hydraulic land reclamation of former parts of the lagoon wetlands (Frascaroli et al., 2021), and land subsidence locally exceeding 1 cm/year (Tosi et al., 2000, 2016). Soil elevation ranges from −4 to −1 m above

sea level (m a.s.l.), which poses a hydrogeological risk of flooding and groundwater salinization (Da Lio et al., 2015; Tosi et al., 2022), and may impact the environment and economy (Torresan et al., 2012).

The water table is kept below sea level through an intricate system of reclamation canals and pumping stations. These facilities drain excess water into the lagoon, rivers, and sea, leading to a seasonal water table fluctuation between 0.4 and 0.8 m below the ground surface (m b.g.s.). The Casetta Pumping Station (CPS, Fig. 1b) and the Cà Bianca Pimping Stations (CBPS, Fig. 1b), operating at the study site (De Franco et al., 2009), are hydraulic structures managed by the Adige Euganeo Reclamation Consortium, the authority responsible for the drainage and management of the irrigation network of the low-lying farmlands between the Bacchiglione (BaR) and Adige rivers. The Brenta (BrR) and BaR rivers flow together with the Morto Canal (MC) between the study site and the lagoon. These three watercourses join near the study site and flow into the sea through a single mouth. At the confluence, the MC mouth is equipped with a system of sluice gates (Vincian gate in Fig. 1) to prevent tidal intrusion.

Since 2020, the mobile barriers (MoSE, i.e. the Italian acronym for Experimental Electromechanical Module), built to prevent the flooding of Venice due to exceptionally high tides (Umgiesser, 2020), have been in operation. When the barriers are raised to close the inlets, the water dynamic in the lagoon changes completely (Ghezzo et al., 2010). This adds anthropogenic forces to the already complex signal of tidal fluctuations in the hydrological system.

From a geological point of view, Late Pleistocene and Holocene sedimentary deposits characterize the subsurface. The Pleistocene sequence, associated with the Last Glacial Maximum (LGM) and a sea-level lowstand, includes alluvial sands, silts, and clays deposited when the sea level was approximately 110–120 m lower than current levels (Donnici et al., 2012; Storms et al., 2008). The uppermost Pleistocene aquifer is formed by fluvial sands capped by an extensive aquiclude of overconsolidated clayey deposits (i.e. Caranto), a paleosol (Donnici et al., 2011).

The Holocene depositional units begin with a thin sedimentary sequence reflecting marine transgression, including back barrier deposits. Overlying this, a sequence associated with the marine highstand depicts the progradation of fluvio-deltaic systems, including prodelta, delta front/littoral, and delta plain/lagoon deposits (Tosi et al., 2009a; Zecchin et al., 2009). The phreatic unconfined aquifer is hosted in littoral deposits on a regional scale and localized paleochannel and ancient littoral ridge systems (Carbognin and Tosi, 2002). The phreatic aquifer is generally composed of alternating sandy and silty layers, the total thickness of which varies from 15 to a few meters in the study area.

The regional flow in the deepest part of the phreatic aquifer is generally oriented from NW to SE (Gattacceca et al., 2009), but horizontal and vertical lithologic heterogeneities strongly influence it locally. The upper part, on the other hand, is mainly controlled by the hydraulic reclamation system, which directs the flow to the drainage canals and pumping stations.

2.2. Data collection and processing

The Venice coastal plain and its surroundings (Fig. 1) are constantly monitored by a network of stations that includes: i) mareographs at Chioggia Vigo (CV) representing the Venice lagoon stage and the Chioggia Diga Sud (CDS) representing the Adriatic Sea

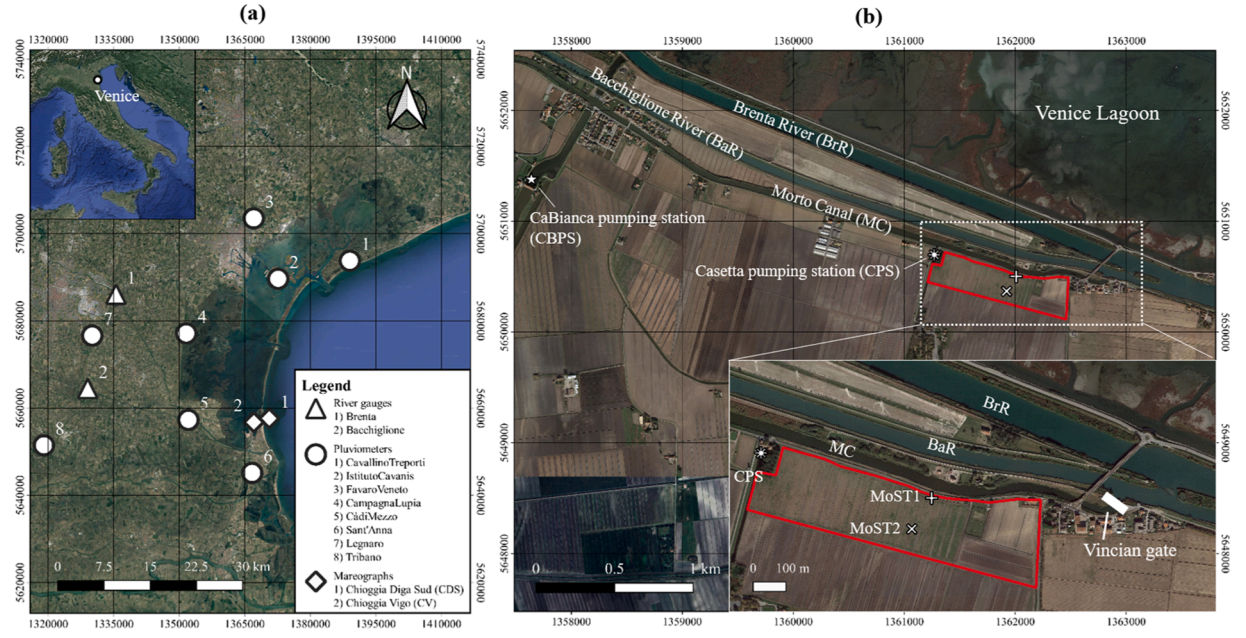

Fig. 1. (a) The Venice coastal plain and its surroundings with the location of the monitoring points including river gauges, pluviometers, and mareographs. (b) The study area with the locations of piezometers (MoST1 and MoST2), surface water bodies (BrR, BaR, and MC), and pumping stations (CBPS and CPS).

stage; ii) seven different rain gauges covering the entire coastal area linked with the Venice lagoon; iii) river gauges at Strà and Bovolenta accounting for BaR and BrR stages. Sea and lagoon level data were retrieved from the ISPRA Veneto monitoring network (https://www.venezia.isprambiente.it/rete-meteo-mareografica), while rainfall and river stage data were downloaded from ARPA Veneto website (https://wwwold.arpa.veneto.it/arpavinforma/bollettini).

The monitoring network set up by IGG-CNR in the field (Fig. 1b) includes different piezometers equipped with CTD Divers® logging sensors measuring water levels (accuracy ±0.5 cm), temperature (accuracy ±0.1 °C) and electrical conductivity (EC) (accuracy ±1 % of reading) with a temporal resolution of 10 minutes. Piezometric heads (m a.s.l.) were calculated via barometric compensation using a BARO-Diver® and referred to the Italian geodetic datum. Unfortunately, in many cases, instrument maintenance, along with blocks and failures of the transducers installed in the field end up in many missing data, which results in a little overlapping of the measurements and limited temporal consistency of the series. This limitation, if not tackled via rigorous data processing, may prevent the use of statistical analysis in the time and frequency domain.

A continuous series of 120 days (January 24th to May 24th, 2022) has been selected for the piezometer MoST1, as the longest time series available, with no missing values or gaps. In the same period, a continuous series of only 38 days (January 31st to March 10th,

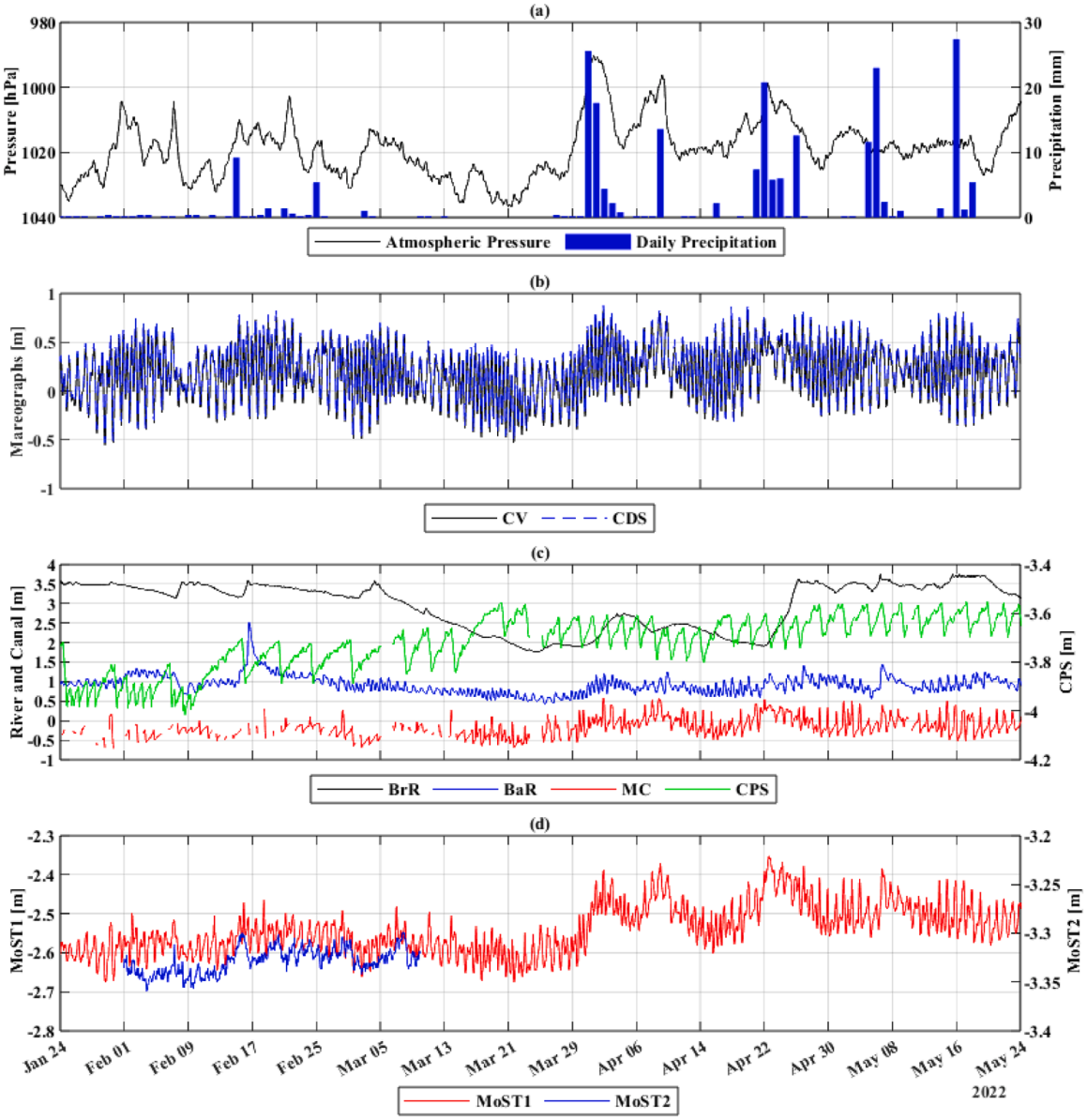

Fig. 2. Time-series records: (a) atmospheric pressure and daily precipitation, (b) water levels recorded at CV and CDS mareographs accounting for the lagoon and open sea stages, respectively, (c) BrR, BaR, MC (left y-axes), and CPS water levels (right y-axes) recorded at Strà, Bovolenta, Cà Bianca, and Casetta pumping stations, respectively, and (d) groundwater levels monitored at MoST1 and MoST2 piezometers.

2022) was available for the piezometer MoST2 (Fig. 1b). Even if shorter, this second set of groundwater data allowed for signal attenuation estimates through the porous media.

As shown in Fig. 1b, to understand such a complex hydrological system and characterize the major driving forces influencing the aquifer flow under the agriculture field, a much larger area was investigated, obtaining a 3-year time series (January 1st, 2020 to December 31st, 2022) of the surface water level fluctuations at MC (i.e. recorded at Cà Bianca Pumping Station, CBPS) and the relative water level oscillation in the drainage system due to the regular pumping cycles (i.e. recorded at CPS). Data accounting for the precipitation, rivers, sea and lagoon levels were downloaded for the same period (Fig. 1a). Seven different rain gauges were interrogated to retrieve a precipitation dataset covering the entire coastal area linked with the Venice lagoon (Fig. 1a).

Furthermore, records of river stages at BaR were retrieved from Bovolenta rain gauge located around 20 km inland, while river stages accounting for the BrR were downloaded from Strà river gauge located around 30 km inland (Fig. 1a).

Tidal data from CV and CDS mareographs, inside and outside the lagoon, respectively, were retrieved from the tidal gauge network of the Venice lagoon. Water levels in the Venice lagoon were monitored by floating tide gauges with simultaneous real-time transmission via VHF radio bridge and GSM (sampling frequency of 1 h).

To allow the coherent processing of those datasets in time and frequency, the series were aligned and synchronized, and the original records were resampled at a fixed 1-hour interval using a Doodson filter (Pugh, 1987). The synchronization and resampling of data

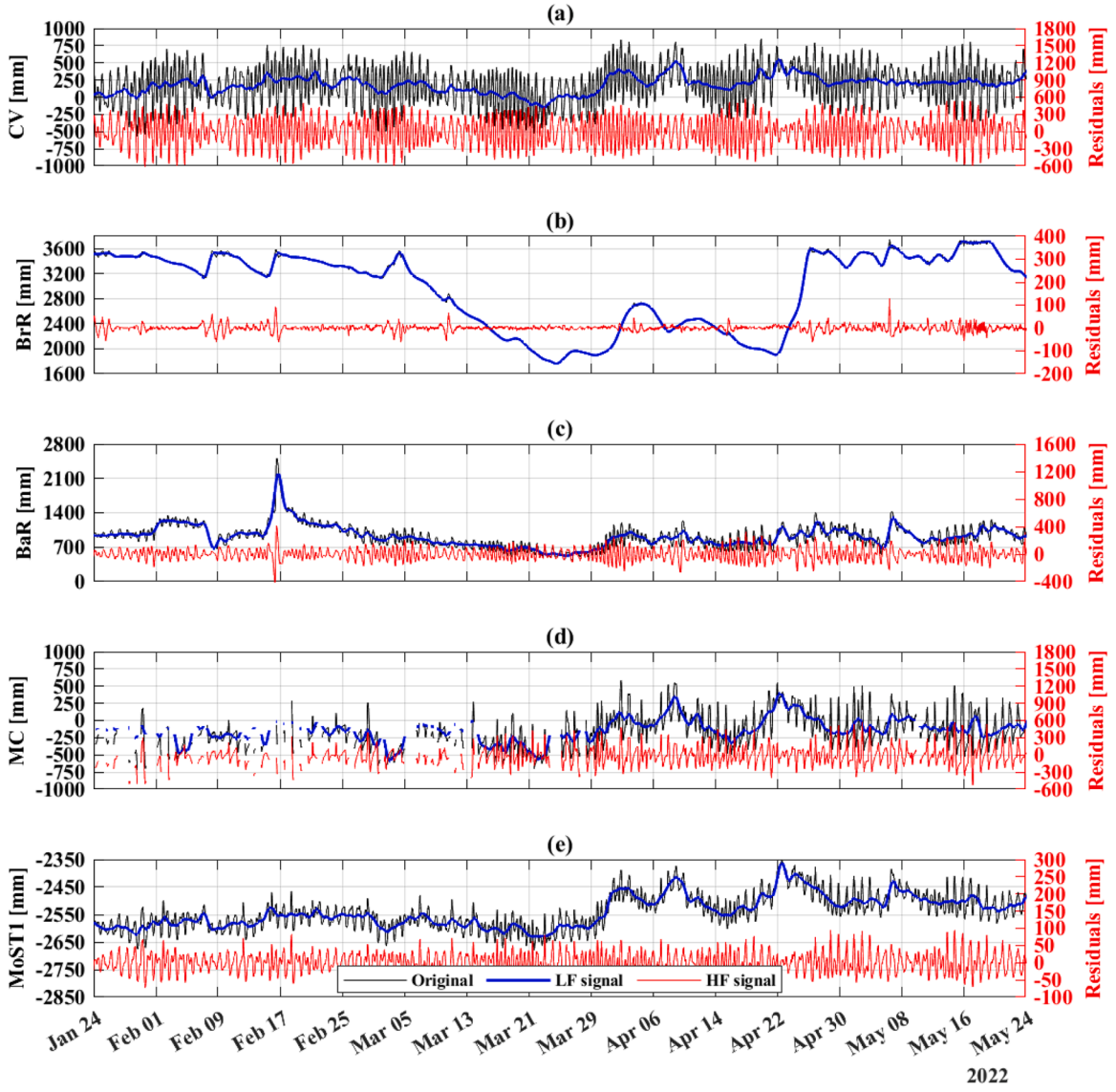

Fig. 3. Comparative plot of raw data (black lines), the Low Pass 33 filter signal (blue lines), and high frequencies residuals (red lines) for (a) lagoon levels at CV, river stage at (b) BrR, and (c) BaR (d) water level in the MC, and (e) groundwater level at MoST1 in the 120-day period. The residual signal was analysed with U_TIDE to assess astronomical tide influence on the water table.

guarantees uniform temporal resolution across the dataset, allowing for consistent interpretation and analysis. Then, a congruence analysis was carried out to identify potential errors, peaks, and noise within the dataset. Such an analysis involved a rigorous examination of the data for anomalies and irregularities that could affect the accuracy of the subsequent hydrological assessments. The elimination of errors, spikes, and noise ensures that subsequent hydrological assessments are based on accurate data, enhancing the validity and reliability of the research findings. The results of those initial pre-processing steps are provided in Fig. 2, which shows in a coherent and neat format all the time series used in the analysis, demonstrating the effectiveness of the data pre-processing techniques in improving the quality and reliability of the dataset.

2.3. Time-series analysis

Understanding the nature of surface- and ground-water level fluctuation is a very complex task and it requires applying advanced mathematical and statistical methods. To assess the correlation between variables of different natures, a strictly statistical approach was followed computing in a MATLAB environment (MathWorks Inc., 2023) Pearson (i.e. linear correlation), Kendall, and Spearman (i.e. non-parametric tests for statistical dependence) coefficients. Such a correlation analysis allowed for the measurement of the strength and direction of association between two variables. Values of ±1 indicate a perfect degree of association between the two variables. As the correlation coefficient value goes towards 0, the relationship between the two variables will be lower. The direction of the relationship is denoted by the sign of the coefficient with the + and – signs indicating a positive and negative relationship, respectively.

To allow a more targeted characterization of each mechanism and a better understanding of the hydrological system dynamics, a high- and a low-frequency (LF) component within each time series were identified, accounting for processes occurring at different time scales. A Low Pass 33 filter tool (LP33) was applied (Emery and Thomson, 2004) on signals representing either Venice lagoon, BaR, BrR, MC, and both piezometric levels MoST1 and MoST2. This filter allowed to dissect each signal and discern between phenomena that occur within (i.e. high-frequency component, red lines in Fig. 3) and beyond (i.e. low-frequency component, blue lines in Fig. 3) 33 hours, distinguishing amongst distinct temporal patterns and mechanisms within the dataset. As the main periodic contribution embedded in each signal was assumed to occur within 33 hours, a harmonic component analysis was performed using a MATLAB-based U_TIDE code (Codiga, 2011) on the high-frequency signal. It is worth stressing that this assumption was tested by running the routine also over the whole signal instead of just the high-frequency part to be able to cross-check the overall accuracy.

This analysis through U_TIDE aimed to separate any tidal influence from other aperiodic contributions and was performed over the entire 3-year dataset to precisely identify the main tidal constituents. The harmonic component builder facilitated the identification of the signal contribution at tidal frequencies from time series, including groundwater records. Having multiple years of data available, representing the variation of the water level in the lagoon and thereby the tidal forcing signal, was fundamental to obtain a robust picture of the significant tidal constituents for the whole system. Such information can be then extrapolated and contextualized also for the shorter time-series related to the two piezometers. All the MATLAB strings are available in the Supplementary Information.

The significance of each component was attributed to the amplitude of the signal, based on the accuracy of the sensors and the signal-to-noise ratio (SNR) with a modified Rayleigh criterion, while their relative importance was controlled by the Percent Energy (PE) contributing to the signal reconstruction (Codiga, 2011). A minimum SNR of 6 and PE of 0.5 % were adopted in this work.

In addition, to understand how the tidal signal propagates and attenuates within the hydrogeological system, a comparative analysis was also performed. U_TIDE was run on each signal for the same 120-day period of the MoST1 piezometer to avoid including non-representative phenomena and focus on comparable datasets. Differences in amplitude and phase of the main tidal components between the signal in the lagoon and all others were also calculated. The comparison of high- and low-frequencies of all the time series in the 120-day period is shown in Fig. 3, which allows to appreciate the differences in amplitude and time scales of the signals.

To further differentiate amongst phenomena occurring with simple low-frequency (LF, beyond 33 hours) and very-low-frequency (VLF, beyond 35 days), an additional filter based on locally weighted linear regression was applied to the low-frequency signal by using 'RLowess' MATLAB toolbox. Such a toolbox defines a regression weight function for the data points contained within the span. This approach allowed to distinguish between different long-lasting driving forces and further focus on "slow" phenomena occurring at different temporal scales, helping in discerning the impact of precipitation and other multi-weekly frequency phenomena occurring over longer periods (e.g., slow and aperiodic sea water level fluctuations, also called meteorological tides by oceanographers).

To calculate residence times in the aquifer, the linear distance among different features (rivers, lagoon, canals, drainage channels, and piezometers) was employed and divided by the average groundwater flow velocity. Considering the Darcy's law in the form of:

$$v = \frac{k * \overrightarrow{i}}{n_e} \tag{1}$$

v is the average groundwater velocity ($L\,T^{-1}$), k is the hydraulic conductivity, $\overrightarrow{i}$ is the equivalent freshwater head gradient ($L\,L^{-1}$), and n_e is the effective porosity (L^3L^{-3}). k was measured via constant head permeameter in triplicate samples on core samples collected in both MoST1 and MoST2. $\overrightarrow{i}$ was calculated using average heads and salinities in the monitored period. n_e was estimated to be on average 0.25 then a minimum value of 0.15 and maximum of 0.30 were used to account for its variability in fine sands (De Marsily, 1986). Finally, to better understand the influence of the various sources of salinity on the aquifer, EC signal was analysed in both monitoring wells and compared with the porewater EC profiles determined on the core samples. To delineate the vertical distribution of salinity at MoST1 and MoST2, the sediments already analysed by Alessandrino et al. (2023) were re-sampled using a 5TE Decagon TDR that measures the volumetric water content, temperature, and bulk EC of sediments. Bulk EC was then converted into porewater

EC using the Hilhorst (2000) relationship, then considering the estimation error of ±3 % in volumetric water content, ±1°C for the temperature, and ±10 % of Bulk EC as provided by the 5TE User Manual, the EC porewater minimum and maximum error was computed for each sample analysed.

3. Results and discussions

3.1. Drivers of groundwater fluctuations

As summarized in Fig. 4, by using a systematic temporal comparison and statistical correlation of the time-series, it was observed that groundwater levels of MoST1 are mainly controlled by the surface water elevation recorded at Cà Bianca (MC), while MoST2 is heavily impacted by the pumping cycles of Casetta (CPS).

The time-series related to the two piezometers (MoST1 anad MoST2) were plotted together with the signals recorded at Cà Bianca (MC) and Casetta (CPS) pumping stations, assessing the statistical correlation of the four series. The strong similarity of water level records at MC and MoST1 was initially observed and investigated. This observation is particularly significant given the proximity of the MoST1 piezometer to the canal, situated at only 29 m. Accordingly, Pearson, Kendall, and Spearman correlation coefficients were

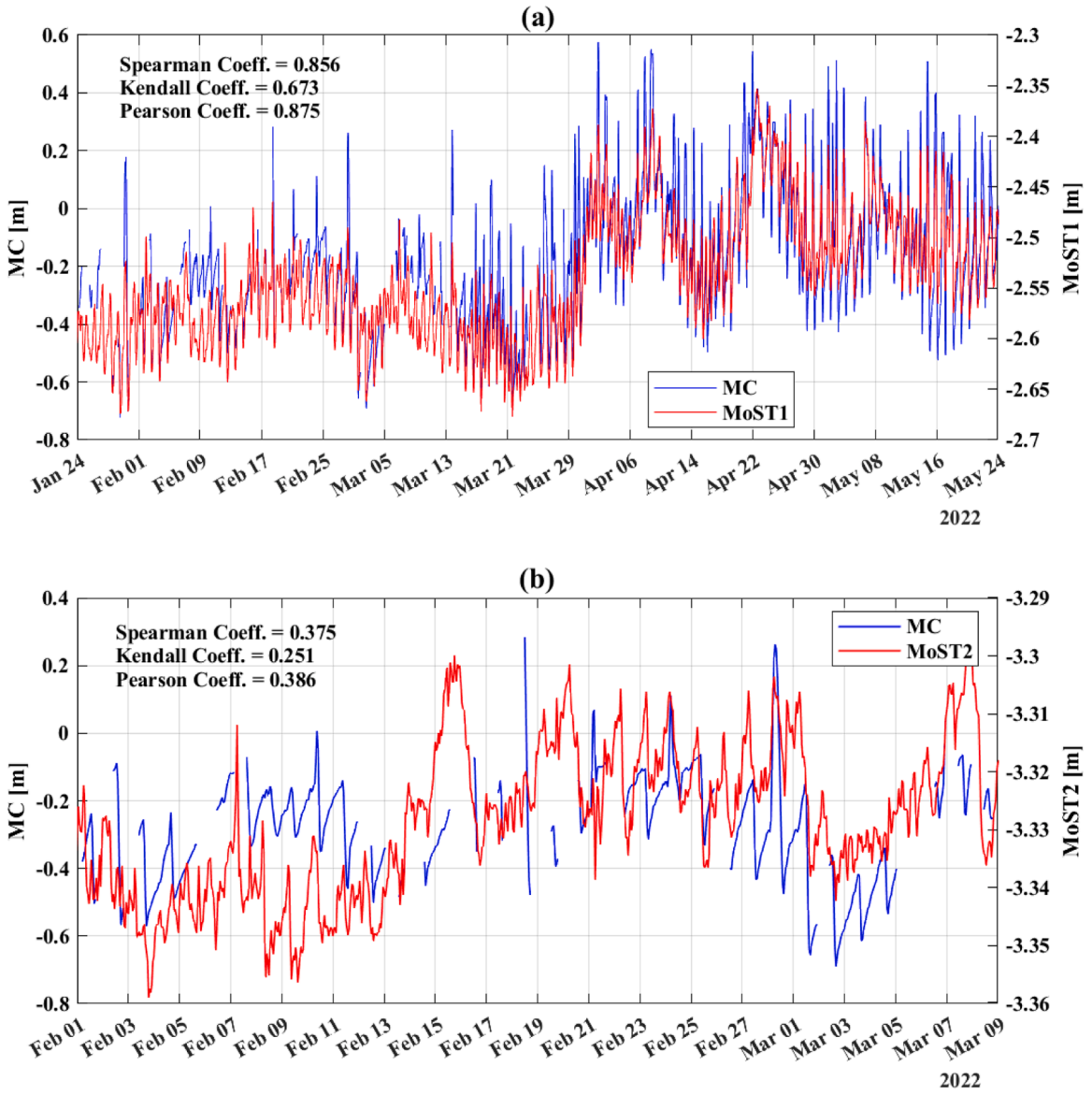

Fig. 4. Comparison plot and Statistical correlation between (a) MC and MoST1 for the 120-day time series, or (b) MC and MoST2 for the 38-day time series.

computed between the canal and the aquifer. As expected, a strong positive correlation was identified between the water level at MC and MoST1 (Fig. 4a). Such a result confirms that the canal and the aquifer are hydraulically connected and, since the water level in the canal has a higher hydraulic head if compared to groundwater, the canal was constantly supplying water to the aquifer. Conversely, all correlation coefficients decrease in the assessment of the signal at MoST2, located at a greater distance (139 m) from the canal (Fig. 4b). The reduction of correlation between MoST1 and MoST2, and MC was much higher than expected, with all coefficients decreasing from MoST1 to about 1/3 at MoST2, in about 110 m of distance. This suggested the concurrence of a different mechanism at MoST2, which may be masking the signal from the canal.

Given that the aquifer is unconfined and the water table very shallow it is reasonable to speculate that precipitation may be a major driver of groundwater fluctuations. Northern Italy was hit by a long period of drought throughout 2022 (Straffelini and Tarolli, 2023), thus clearly isolating the precipitation response from the rest of the signals on the available time series wasn't possible due to lack of precipitation events during the monitoring period (see Fig. S1 in Supplementary Information).

A strong positive dependency was observed between MoST2 and fluctuations at CPS (Fig. 5b), much stronger than the correlation between the pumping cycles at CPS and MoST1. The reason for this outcome lies in the location of the dense network of drains and trenches in the field. That network contributes to maintaining the groundwater level below the surface by draining the water exceedances out, via the pumping cycles of Casetta (CPS). It should be noted that, while MoST2 is located around 50–80 cm far from a

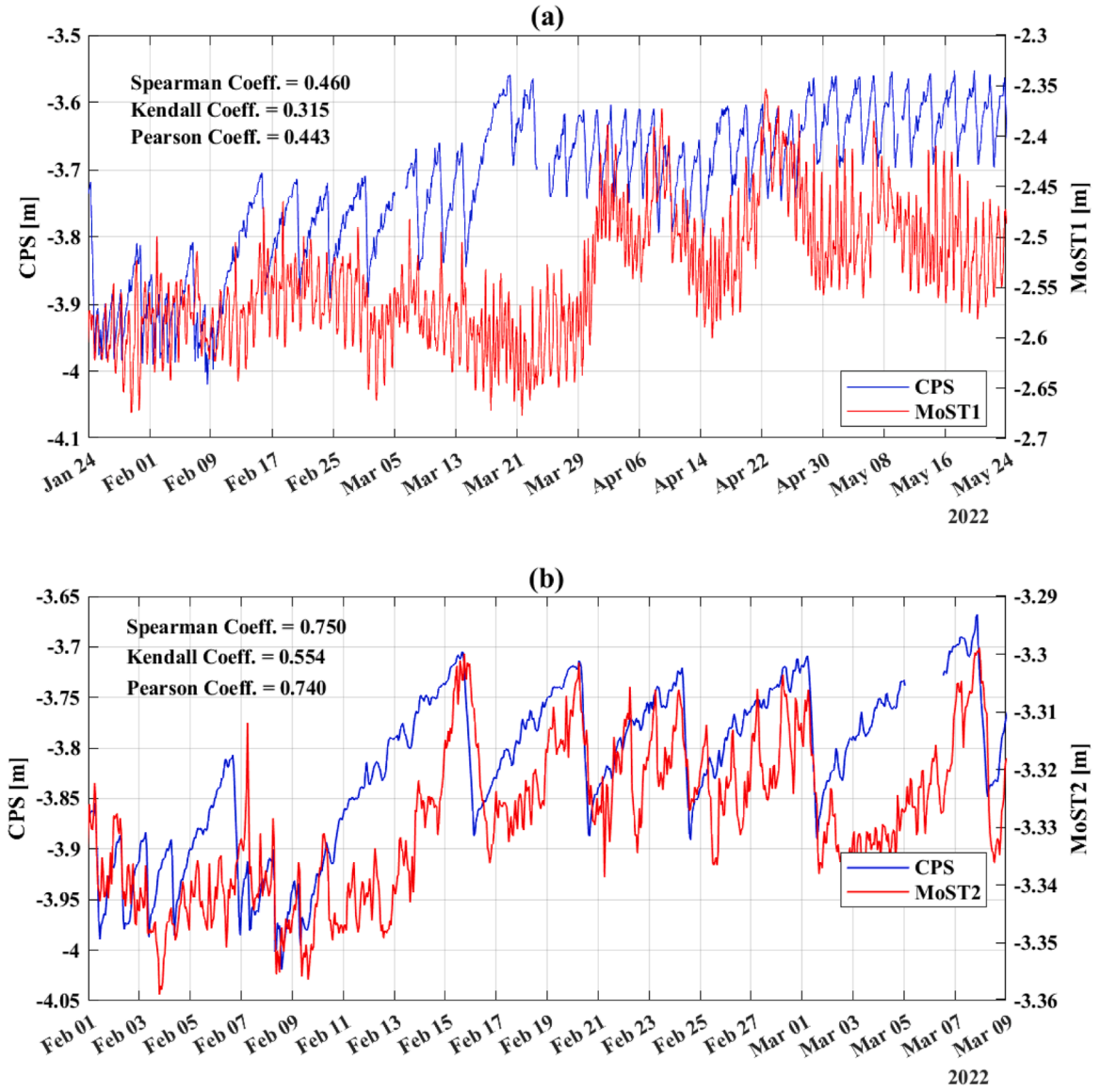

Fig. 5. Comparison plot and Statistical correlation between (a) CPS and MoST1 for the 120-day time series, or (b) CPS and MoST2 for the 38-day time series.

drain, MoST1 is not in proximity to one of those drains.

Such a result highlighted the importance of carefully considering the piezometers and sensors' positioning when building up a monitoring network, since it could affect the analysis leading to misapprehended conclusions on how the aquifer system works. Other factors like mechanical loadings due to vehicles were excluded since the zone is rural with very low vehicular traffic. While atmospheric pressure was negatively moderately correlated with the groundwater level (see Fig. S2 in Supplementary Information); this can be explained by the inverted barometric effect in the Adriatic Sea that in turn affects groundwater levels coastal unconfined aquifers (Balugani and Antonellini, 2011).

Finally, the observed low correlation between MC and the southern part of the aquifer, in the centre of the field cannot be attributed

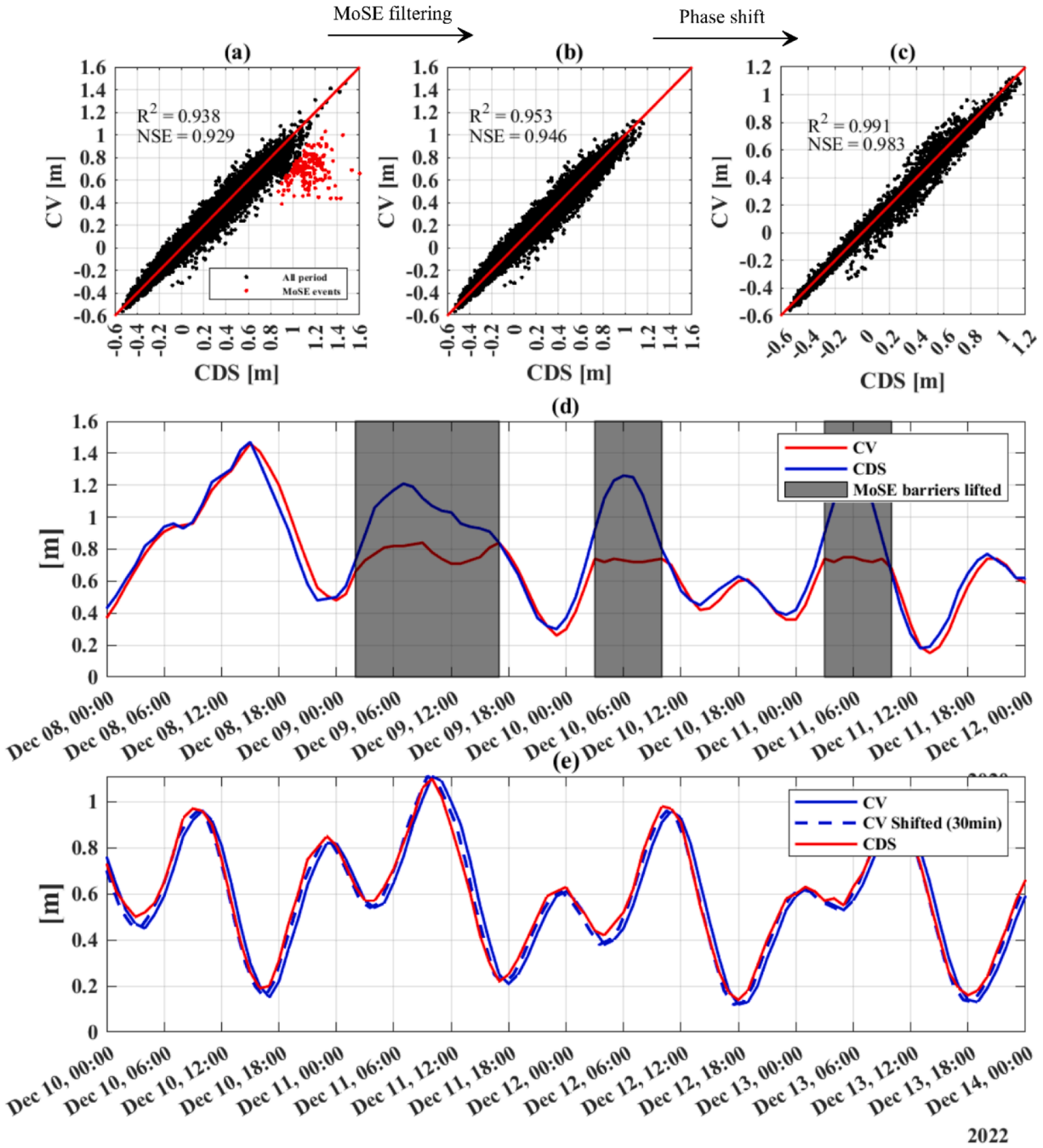

Fig. 6. Head Scatter Diagrams of CDS and CV mareographs (a) before, (b) after filtering out MoSE events, and (c) after phase shifting. (d) depicts head fluctuations highlighting differences between the mareographs due to MoSE barriers lifting (vertical grey bands). (e) depicts head fluctuations highlighting a better alignment between the mareographs due to the shifting procedure.

to a lack of connection between the canal and the aquifer system as previously postulated by Lovrinović et al. (2021), but it is mainly a side-effect of the local impact of pumping cycles (transmitted by the drains) on MoST2, which is "hiding" the underlying signals.

3.2. High-frequency signal analysis and tidal influence assessment

The analysis identified the main five components (O1, K1, N2, M2, S2) of the astronomic tides that describe most of the signals at high frequency in the system, which is something still observed at 20 km inland along the river (BaR). Looking at the aquifer, the signal at MoST1 is highly impacted by the tide influence (i.e. 76.1 % of the high-frequency signal), probably driven by the water table variation within the canal nearby (MC).

To verify the robustness of the data representing the boundary condition of the domain, the time series recorded by the two

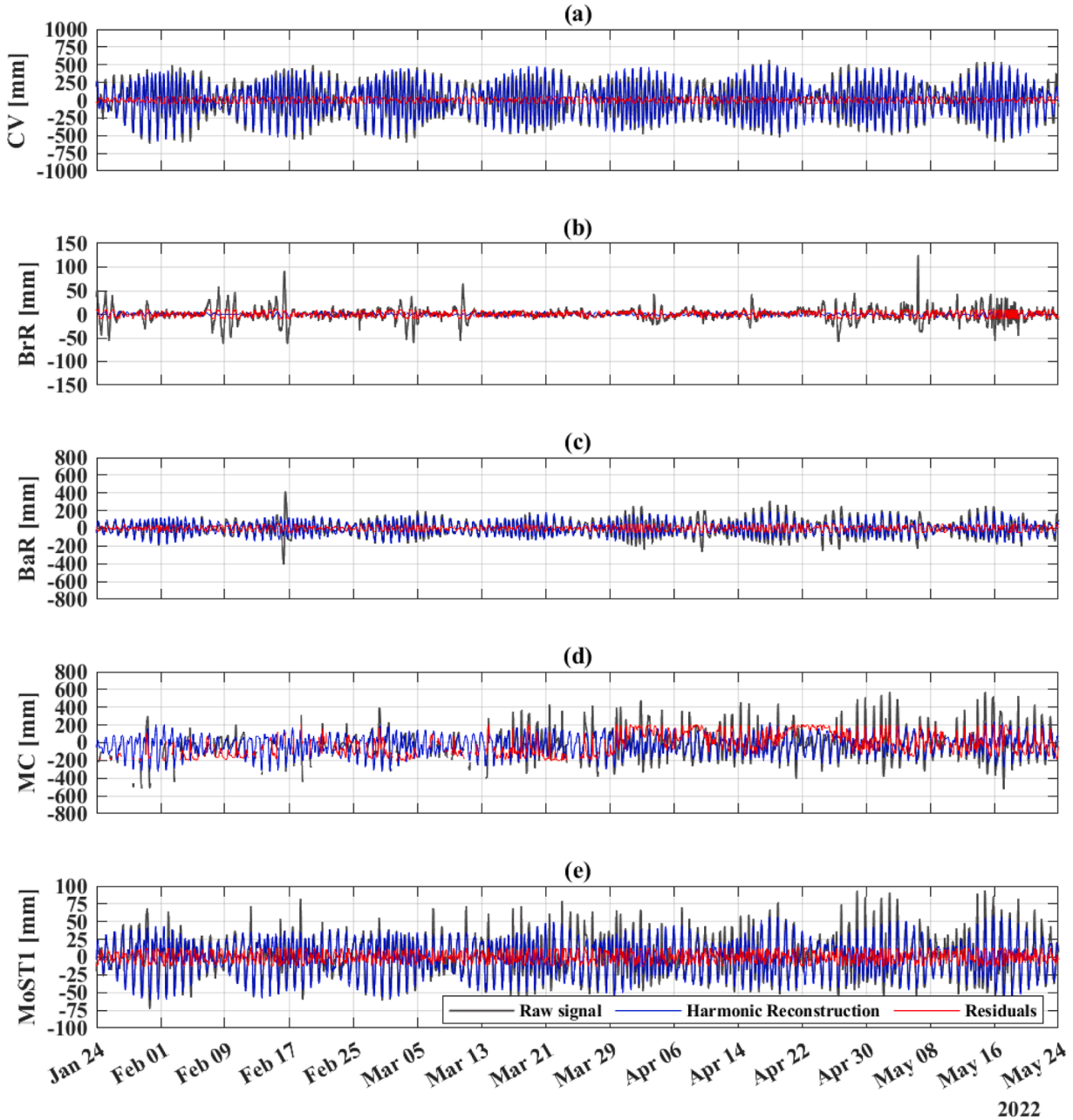

Fig. 7. Signal reconstruction by harmonic components of (a) CV, (b) BrR, (c) BaR, (d) MC, and (e) MoST1 high-frequency signal. In each graph, a comparison of raw high frequency records (black lines), tidally reconstructed signal (blue lines), and non-tidally explained residuals (red lines) is shown.

mareographs (CV and CDS) were tested to find potential differences between the signals and assess the tidal stresses in the study.

High Adriatic Sea water events requiring the intervention of MoSE floating barriers (as published in the official bulletin) were filtered out to limit such signal disturbances in the harmonic decomposition analysis (Fig. 6). This procedure ensured the removal of noise and irregularities, which would have made the harmonic decomposition analysis highly biased. This is something that needs to start being considered in environmental studies in the region. It is worth stressing that to avoid subjective cut-off of data, in the case of MoSE activation, the full day was removed from the series.

In addition, given the distance of the two sea gauges, a sub-hourly delay between the two signals was supposed. Thus, a 30-minute shift over the signals was identified as the best phase shit maximizing the correlation between the records of the two mareographs (Fig. 6c). Since after these pre-processing, the signals resemble one another (Fig. 6e), CV mareograph was selected to represent tidal forcing inside the Venice lagoon, being more directly connected with the area.

The astronomic tide assessment on the high-frequency residuals allows a quantitative assessment of tidal influence on Venice lagoon, BaR and BrR, MC and both MoST1 and MoST2 time series. Out of 68 harmonic components (astronomical period components), identified in the analysis of 3-year-long signals, only five resulted to be relevant, when applying significance limits (i.e. SNR = 6, PE > 0.5 %). Those five components bring most of the information and describe most of the variability of the signal in the mareograph and were, thereby, used to reconstruct the signals (as summarized in Fig. 7): O1 (effect of the moon's declination); K1 (main lunar diurnal constituent); N2 (non-circularity of the moon's orbit); M2 (main semidiurnal lunar constituent); S2 (main semidiurnal solar constituent).

U_TIDE allowed the generation of reconstructed superposed harmonic fits (blue lines in Fig. 7), estimating the percentage of signal described by selected tidal constituents (Codiga, 2011). Such a quantitative estimation for this area was not performed in previous studies and represent a critical aspect to build a credible conceptual model. The analysis showed that 91.8 % of the high-frequency record in the Venice lagoon is explained by these five constituents, while the other 8.2 % is due to other minor periodic components and aperiodic meteorological forcings. In the same way, astronomical tide components explain 68 % of the high-frequency BaR signal. Considering that data were recorded at the Bovolenta river gauge, located approximately 20 km inland from the study area, the observed tidal influence on the BaR time-series is quite remarkable, even though the amplitude of the high-frequency signal at the location is only about ~10–20 cm. The same cannot be said for the BrR, where the tidal influence diminishes drastically, and the periodic components describe just 3.7 % of the river's high-frequency signal. For MC, this percentage is 49.3 %. The time series was collected from the Cà Bianca pumping station (CBPS), which is slightly more inland than the field trial. Moreover, the presence of hydraulic structures (e.g., Vincian gates in Fig. 1) that introduce noise into the signal may have reduced the tidal influence estimate. On the two piezometers (MoST1 and MoST2), astronomical tide components explain 76.1 and 61.5 % of high-frequency signals, respectively. The higher percentage of tidal influence on the signal of the closest piezometer to the lagoon suggests that only a part of the tidal perturbation in the Venice lagoon influences the water head in the inland piezometers. This large proportion of high-frequency signals attributed to astronomical tides in both piezometers highlights the importance of considering tidal effects when analysing groundwater dynamics in coastal areas. It is worth stressing that the significant constituents were found using a 3-year time series, while the comparison between different signals was performed over a period of 120 days to avoid including non-representative phenomena that could affect the assessments (e.g., storm surge, floods). Furthermore, the analysis only describes high-frequency signals, which are embedded into an overall signal recorded by the devices. Necessarily, these must be contextualized in relation to the amplitude of the original time-series, which represent the energy of the total water-level signals. The percentage of the signal of the mareograph (CV) described by periodic constituents drops from 91.8 % to 77.5 % considering the whole original signal instead of only high frequency. This means that 77.5 % of the whole signal recorded by the mareograph in 3 years can be described by only 5 periodic components of the astronomic tide, while 22.5 % represents different aperiodic stresses on water levels. Even if this percentage is still quite high, such a reduction underlines the importance of using an LP33 filter and focusing on high-frequency components to effectively grasp tidal contribution on each signal and properly assess the more relevant harmonic components. At BaR, this percentage drops from 68 % to 14.7 %, which was something expected given the wide difference in the amplitude of the signals at high and low frequencies in the river. Such a difference results from the impulsive and transient nature of phenomena occurring at lower frequencies in a river, such as flood events, which completely overcome the little period mechanisms. At BrR, the percentage goes from 3.8 % to 2.5 % considering the full original signal. MC goes from a percentage of 49.4–40.8 %. MoST1 goes from 76.1 % to 39.1 %, while MoST2 goes from 61.5 % to 36 %. Although the signal percentages described by astronomical tidal constituents is almost halved in both piezometers focusing on the original signals, the tidal influence remains not negligible in comparison to the other aperiodic forcings. In fact, considering a total range of variability of 323.3 mm, the absolute value of the reconstructed signals varies between 59.3 mm (sygizial tides) and −59.8 mm (quadrature tides). A minor influence can be observed in MoST2, considering a total range of 59.9 mm with maximum and minimum values of 4.32 and −3.97 mm, accounting for sygizial and quadrature tide, respectively.

Table 1 and Table 2 show the amplitude and phase values of each of the five main components identified, in ascending order of frequency. The components characterized by larger amplitudes (and therefore carrying the most energy) in the mareograph installed in the Venice lagoon (CV) are K1, M2, and S2, with amplitudes equal to 152, 229, and 157 mm, respectively. Remarkably, the main semidiurnal lunar constituent (M2) alone describes 50 % of the signal. By looking at those components within the other signals, there is a uniform decrease in amplitudes and a redistribution of the percentages of energy. In the case of MC, for example, the redistribution of energy makes the O1 component more influential for the signal in the canal than it was for the signal in the lagoon. It is also the case of the component K1, whose PE values rise in all the signals compared to the lagoon. Generally, the attenuation of amplitudes is growing moving away from the lagoon, regarding both the surface and underground water bodies. Focusing on the two piezometers, the tidal perturbations decrease moving inwards. MoST2 showed an attenuation rate higher than MoST1, which conserves more amplitude. Moreover, most of higher-frequency components seem to be smoothed out by pressure propagation in porous media, following the

main theory of incompressible flow: the higher the component frequency, the greater the attenuation in a dissipative media. At the same time, MoST2 signal had more phase delay than MoST1 (Table 2). This observation confirms the findings of Mao et al. (2006) and Rama et al. (2018), and is due to the tidal perturbation pathway, which moves from the estuary along the course of the river toward the centre of the domain.

3.3. Low-frequency signals analysis and aperiodic contributions

As shown in Fig. 8, MC turned out to be mainly influenced by meteorological tides, while only partially by BaR slow water level oscillations. Slow and aperiodic water level fluctuations recorded in Cà Bianca (MC) and Chioggia (CV) show remarkable similarities, with very high calculated Spearman, Kendall, and Pearson correlation coefficients. Conversely, slow river levels oscillations (i.e. BaR VLF signal) are only partially transmitted to the canal (MC), with a clear decrease of all the correlation coefficients. Discerning temporal patterns and mechanisms within the signal was pivotal to gaining a comprehensive understanding of MC signal, which presents a non-negligible number of disturbances (Fig. 2) and mainly controls groundwater levels in MoST1 (Fig. 4).

For these reasons, the residual part of the signal (i.e. Low-frequency) was interrogated to try to distinguish amongst other long-lasting driving forces. The very-low-frequency (VLF) signal in MC was compared with VLF signals of both BaR and Venice lagoon at Chioggia (CV), comparing the slow oscillations in the two water bodies hydraulically connected to the canal (MC). Such a comparison was performed considering the whole 3-year dataset. The correlation analysis revealed a significant positive dependence of the canal on slow water fluctuations recorded in the Venice lagoon with calculated correlation coefficients reaching values from 0.722 to 0.898 (Fig. 8). Conversely, a lower correlation was observed with the BaR signal and coefficients significantly decreased. This could be attributed to the high residual peaks still present after the LP33 filter application on the BaR record, representing prolonged but still impulsive flood events driven by the river, which are usually cut out from the canal by the activation of the Vincian gates.

The relationship between these peaks in the BaR LF signal and daily precipitation events were further investigated. To identify which are the more influential precipitation dataset and select the corresponding rain gauges, the precipitation occurrence in correspondence of flood events registered in BaR was calculated. Multiple rain gauge stations were used (Fig. 1a), residual peaks in BaR were isolated and precipitation occurrence was estimated considering different peak heights and amounts of precipitation. The analysis shows that as the river peak height increases, the precipitation occurrence in each rain gauge also increases. Conversely, with an increase in the amount of precipitation, the precipitation occurrence decreases (see Table S1 in Supplementary Information). The three rain gauges (Pluv.1, Pluv.3, and Pluv.4) with higher percentages of precipitation occurrence in correspondence with flood events were selected as the most representative for the river (BaR). Subsequently, a correlation analysis between the areas underlying each peak and the corresponding cumulative precipitation at the identified rain gauge stations was performed. A reasonably good correlation was found, with the correlation coefficients ranging from 0.556 to 0.766 (Fig. 9a). As expected, the scatter plot revealed an exponential relationship between the cumulative precipitation and the underlying area of the hydrographs (i.e. indirect estimate of the water volume of the flood), as described in Fig. 9b.

By comparing the low-frequency signals in the system, it was possible to isolate the root-causes of the slow oscillation of the water levels in the river (BaR), which are mainly driven by precipitation events that alter the average level for many days. Those variations are only partially transmitted to the canal (MC), which result mainly affected by the upgradient boundary (Venice lagoon at CV) also for the low-frequency signal.

Table 1
Comparative tidal analysis (amplitudes with 95 % confidence interval). Only relevant components (namely SNR $\geq$ 6, PE $\geq$ 0.5 %) were represented.

Tidal component		Venice lagoon			Morto Canal			Bacchiglione River		
Name	Freq[c] (cl./h)	Amp. (mm)	P.E. (%)[a]		Amp. (mm)	P.E. (%)	Atten. (%)[b]	Amp. (mm)	P.E. (%)	Atten. (%)
O1	0.039	47.4	2.14		49.3	11.6	−4.0	4.37	0.2	90.8
K1	0.042	152	22.08		86.3	35.4	43.2	53.7	29.7	64.7
N2	0.079	33.7	1.08		14	0.9	58.5	9.58	0.9	71.6
M2	0.081	229	50.13		78.3	29.2	65.8	62.1	39.7	72.9
S2	0.083	157	23.44		44.7	9.5	71.5	47.1	22.8	70.0
Tidal component		Brenta River			MoST1 piezometer			*MoST2 piezometer		
Name	Freq[c] (cl./h)	Amp. (mm)	Amp. (mm)	Amp. (mm)	Amp. (mm)	P.E. (%)	Atten. (%)	SNR (RM)	ΔPha (h)	ΔPha (h)
O1	0.039	1.24	1.34	1.34	1.34	5.3	83.9	44	−6.6	−6.01
K1	0.042	1.99	3.74	3.74	3.74	41.6	85.9	78	−15.6	−3.86
N2	0.079	0.15	0.03	0.03	0.03	0.9	90.7	0.71	8.74	9.08
M2	0.081	0.58	1.74	1.74	1.74	37.1	91.2	5.6	0.79	8.72
S2	0.083	0.47	1.22	1.22	1.22	11.9	92.7	4.1	0.33	8.31

[a]P.E. is the percent of energy that contributes to the signal reconstruction as the ratio between component energy, gauge of potential energy of sea level, and total energy of the reconstructed signal.
[b]Atten. is the attenuation of the component in comparison of the Venice lagoon signal. It is calculated by 100 minus the ratio of component amplitude in the piezometer and in the lagoon-level gauge.
[c]cl/h means cycles per hour. It is a frequency unit that implies a 1/3600 cl/h for a frequency of 1 hertz.
*MoST2 analysis was performed on the 38-day time series.

Table 2
Comparative tidal analysis (phases with 95 % confidence interval). Only relevant components (namely SNR ≥ 6, PE ≥ 0.5 %) were represented.

Tidal component		Venice lagoon			Morto Canal			Bacchiglione River		
Name	Freq[c] (cl./h)	Pha. (360°)	SNR (RM)[a]		Pha. (360°)	SNR (RM)	ΔPha (h)[b]	Pha. (360°)	SNR (RM)	ΔPha (h)
O1	0.039	52.2	950		87.1	570	−2.50	136	30	−6.01
K1	0.042	60.9	11000		103	1400	−2.80	119	3200	−3.86
N2	0.079	267	470		326	35	−2.07	8.68	110	9.08
M2	0.081	262	20000		308	820	−1.59	9.3	3800	8.72
S2	0.083	271	6900		318	280	−1.57	21.8	2100	8.31
Tidal component		Brenta River			MoST1 piezometer			*MoST2 piezometer		
Name	Freq[c] (cl./h)	Pha. (360°)	SNR (RM)	ΔPha (h)	Pha. (360°)	SNR (RM)	ΔPha (h)	Pha. (360°)	SNR (RM)	ΔPha (h)
O1	0.039	144	44	−6.6	87.3	1000	−2.52	146	130	−6.73
K1	0.042	296	78	−15.6	108	6100	−3.13	110	830	−3.26
N2	0.079	18.4	0.71	8.74	324	130	−2.00	16.9	0.13	8.79
M2	0.081	239	5.6	0.79	311	5100	−1.69	347	180	−2.93
S2	0.083	261	4.1	0.33	316	2600	−1.50	171	120	3.33

[a]SNR (RM): signal-to-noise ratio with modified Rayleigh criterion.
[b]ΔPha: phase delay between the offshore component in the Venice lagoon and the same component in the piezometer (measured in h: hours).
[c]cl/h means cycles per hour. It is a frequency unit that implies a 1/3600 cl/h for a frequency of 1 hertz.
*MoST2 analysis was performed on the 38-day time series.

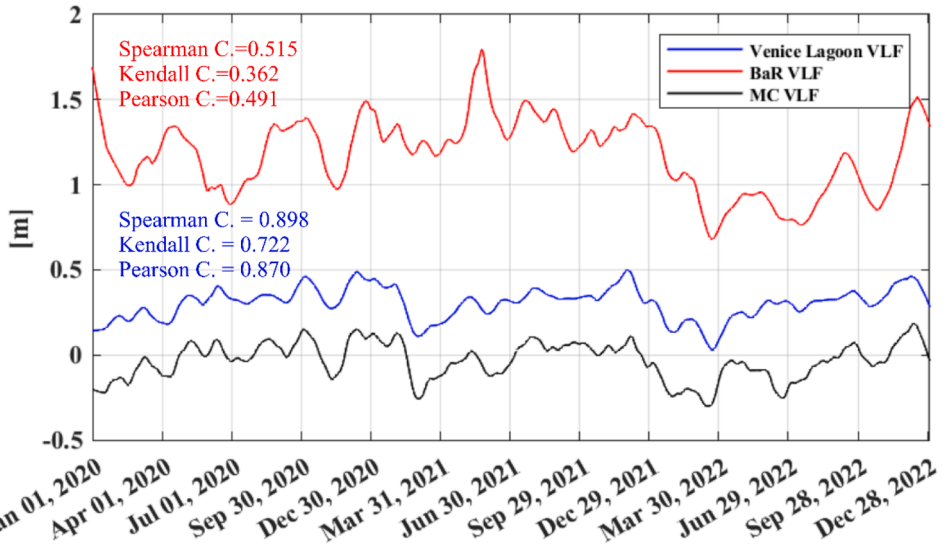

Fig. 8. Correlation analysis between MC and BaR and Venice lagoon (CV), respectively. The analysis was performed on very low frequency signals retrieved by means of the 'RLowess' MATLAB toolbox.

3.4. EC frequency signals analysis

The understanding of the system from a hydrodynamic point of view is of fundamental importance to capture other important dynamics affecting the system. Among these, aquifer salinization stands out as a major issue that is threatening the agricultural production in the study field. In fact, sensors placed on site by IGG-CNR measured very high values of EC reaching maximum of 40 mS/cm (Lovrinović et al., 2021).

With the aim of highlighting challenges and limitations that may arise in understanding salinization dynamics in field trials with similar set-up, the same approach used for the water levels signals was adopted considering the EC signal. Furthermore, EC vertical profiles from porewater were plotted to enrich the analysis and underline complex mechanisms affecting the comprehension of salinization dynamic.

The EC recorded in MoST1 showed a slight negative drift with values between 40.5 and 40 mS/cm (Fig. 10a). In contrast, MoST2 revealed an opposite (positive) trend with values between 8.5 and 11.5 mS/cm (Fig. 10b). Such contrasting values and trends between MoST1 and MoST2 could suggest a strong spatial heterogeneity of the salinity distribution under the field study, related to the distance from the canal (MC), with a minor salinity in the inland piezometer. However, this result is disproved by the EC vertical profiles that, even if they show minor differences between the two piezometers (Figs. 10c and d), do not confirm the horizontal spatial variability suggested by the time series. It is worth stressing that EC values were recorded using data loggers in fully screened wells which prevents inferring the actual aquifer salinity stratification due to intra-borehole mixing processes that could alter, locally, saltwater-freshwater

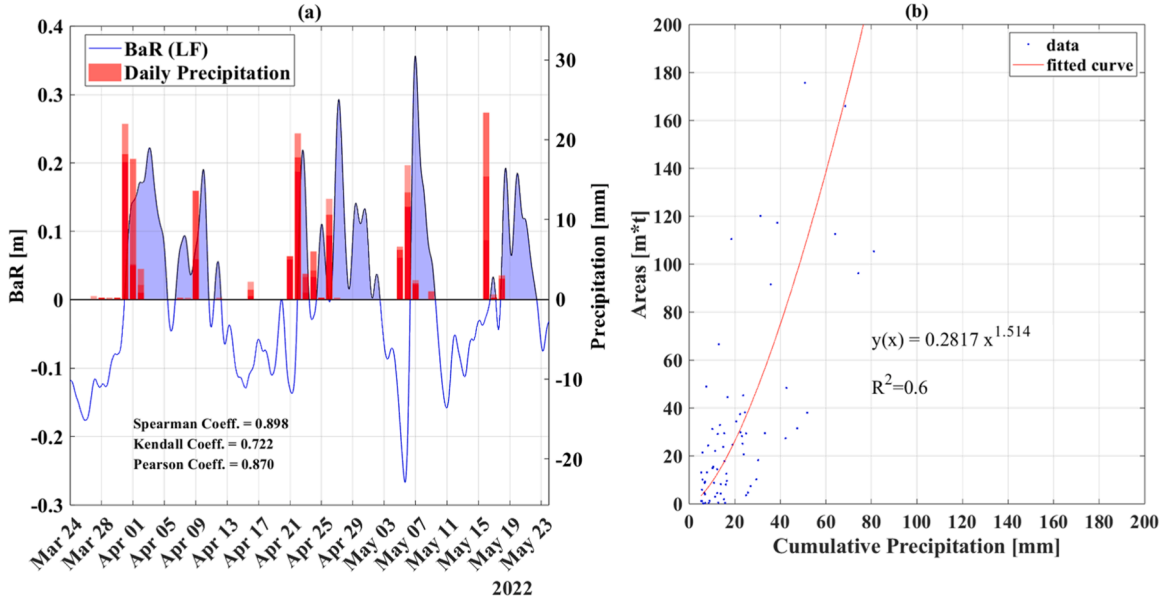

Fig. 9. Correlation analysis between areas underlying each positive peak in BaR signal and cumulative daily precipitation: (a) zoom in on positive peaks and daily precipitation at selected rain gauges; (b) scatter plot of areas and cumulative precipitation with the best fitting curve.

interface and trigger vertical flows within the wells (Alessandrino et al., 2023; Mastrocicco et al., 2012; Shalev et al., 2009). Such a limitation in the EC profiling methodology can be observed in Cavallina et al. (2022), where the EC profiles recorded in both MoST1 and MoST2 indicated a very high variability over the year. Within the upper few meters below the ground surface, the EC values showed strong variations throughout the monitored year: 3–40 mS/cm in MoST1 and 4–35 in MoST2. Moreover, by looking at the EC

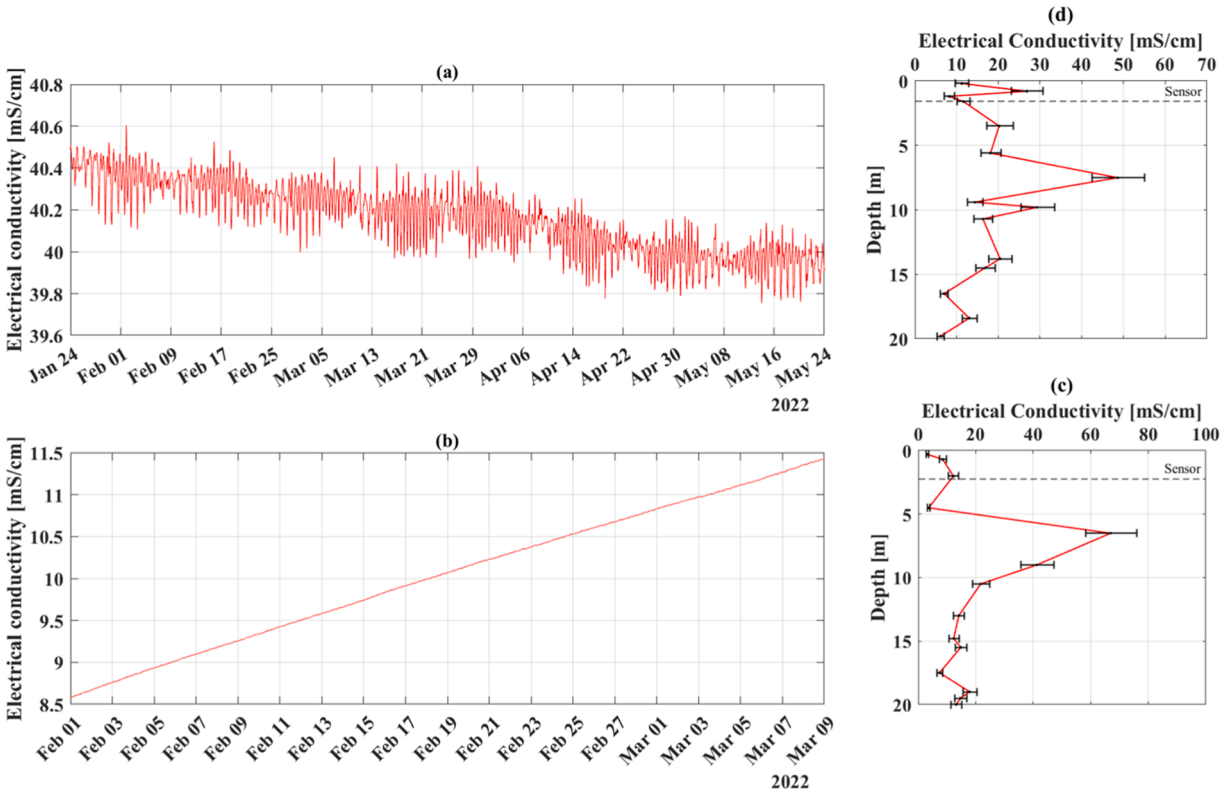

Fig. 10. Trends and profiles of EC recorded at MoST1 (a and c) and MoST2 (b and d) piezometers.

trends and profiles, attributing the variability of salinity in time and space to external forcing such as precipitation, as suggested by Lovrinović et al. (2021), is thoroughly challenging. Instead, this variability seems to be affected by the in-well position of the sensor and the advective-convective mixing processes occurring within the monitoring piezometers, which are to no extent representative of the aquifer system.

However, it was remarkable to observe a clear, although little in amplitude, influence of periodic stresses on the EC signals of MoST1, which is the piezometer closest to the canal (MC). To assess the influence of tidal perturbation on the EC signal oscillations, a harmonic component analysis using U_TIDE was performed on the high-frequency part of the EC signals of the two piezometers, after applying the LP33 low pass filter, in agreement with the approach followed for the rest of the time-series.

As shown by the curves in Fig. 11, the analysis revealed a distinctive tidal influence on MoST1 high-frequency EC records, which is rapidly dissipated throughout the porous media and does not affect MoST2. Accordingly, in MoST1, a remarkable 69.2 % of the high-frequency EC signal is described by the five tidal constituents identified with the previous steps of the analysis, while, using the same components, only 7.1 % of the signal is explained in MoST2. It is worth remembering that, as done for the water elevation signal, these

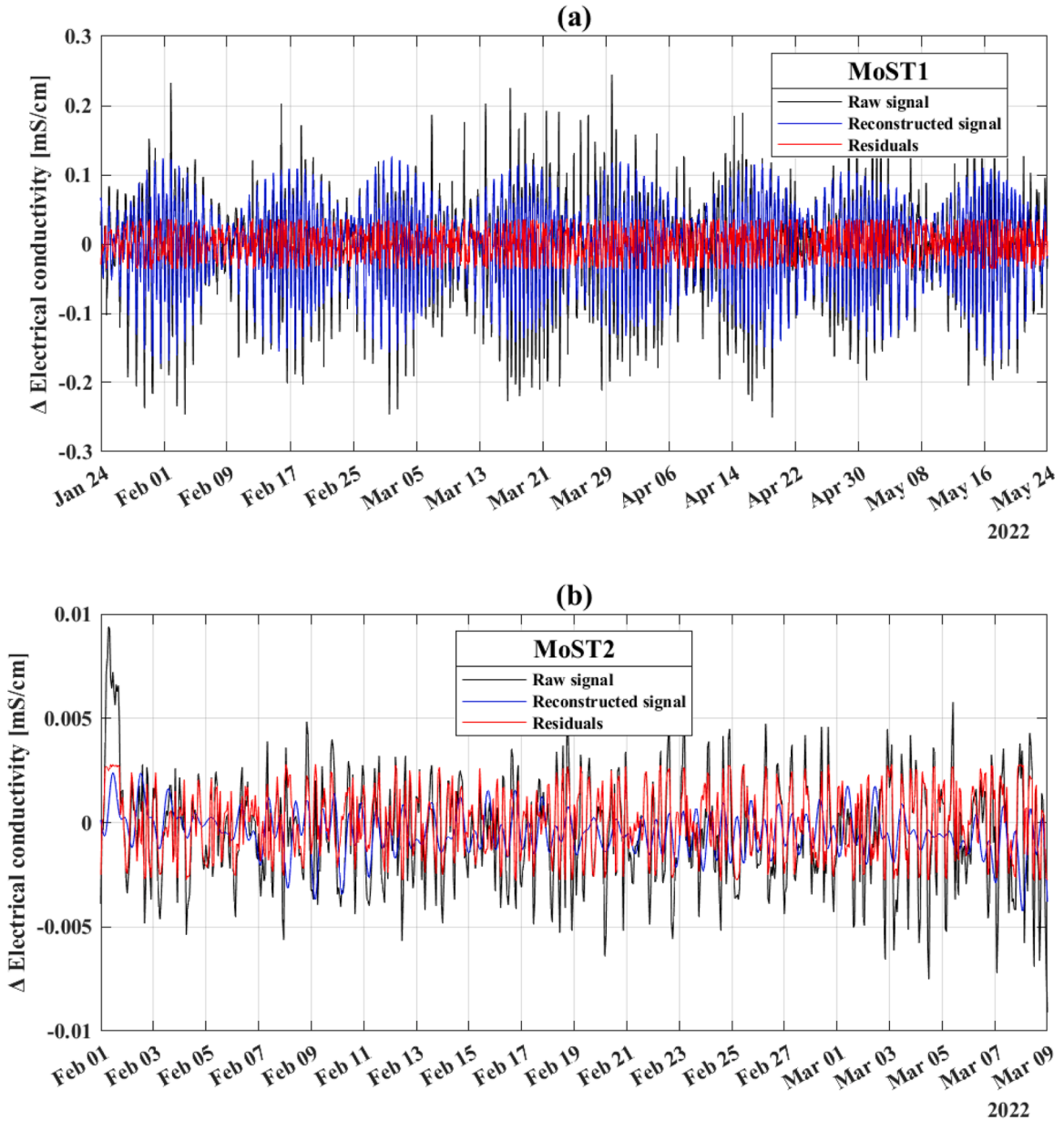

Fig. 11. EC signal analysis of (a) MoST1 and (b) MoST2, reconstructed by tidal harmonic components obtained from U_TIDE. In each graph, a comparison of raw high-frequency records (black lines), tidally reconstructed signal (blue lines), and non-tidally related residuals (red lines) is shown.

percentages need to be contextualized with the amplitude of the original EC signals, which represent the amount of energy transmitted by the mechanisms. High-frequency EC oscillations recorded in MoST1 are within a range of 0.4 mS/cm. Considering a background value of 40 mS/cm, this is roughly 1 % of the signal, which means that tidal forcing cannot be considered as a major driver of salinity distribution in the aquifer. The tidal analysis carried out both on the water levels and EC time series shows that, although from a point of view of the level oscillations the tidal forcing is present and clear, it cannot be considered pivotal in affecting the EC background levels. As stated by Alessandrino et al. (2023), many hydrologic processes are involved in the groundwater salinization dynamics. Moreover, the in-well position of the sensors and the depth of the freshwater-saltwater interface within the piezometers should not be overlooked.

3.5. Conceptual model, residence times and limitations

To describe and summarize the hydrodynamic of the area as it was uncovered by this work, a schematic conceptual model is provided in Fig. 12. The residence times from the Venice lagoon to the piezometers is in the order of 4–5 years. Thus, while piezometric variations are almost coincident with the stage variation in the Venice lagoon, it may take a long time to observe EC variations in groundwater due to surface water bodies influence. On the other hand, the residence time from MC to MoST1 is in the order of a week. This inevitably puzzles the EC observations in the aquifer that are influenced by the varying residence times and unknown EC of all the surface water bodies. In fact while the Venice lagoon and MC are almost always saline throughout the year (De Franco et al., 2009), BrR and BaR can produce significant freshwater input in the aquifer during flood events (Viezzoli et al., 2010). Finally, the residence times from the piezometers to the drainage channel increase again due to the low gradient in the aquifer, consequently the salinity shifts in the reclamation network is also quite delayed and complex.

The approach showed how to make use of data from monitoring networks established for different purposes to improve the understanding about a highly anthropized coastal aquifer. The analysis also identified possible knowledge gaps and challenges to be addressed such as the lack of available EC measurements and vertical discretization along the piezometers at key monitoring points. To address these gaps, a more targeted monitoring approach is needed, including strategically placed sensors to capture salinity in key locations, e.g. as showed in this paper at MC, which have proven to be hydraulically connected and very influential with/for the aquifer system. Although establishing an integrated network of extreme detail is a utopiafor understanding hydrological forces at a regional scale, this study advises the importance of sensitizing the responsible parties to coordinate the next updates and extensions of the monitoring networks. Given the huge influence of little lithological variabilities on the subsoil freshwater-saltwater exchange (Cavallina et al., 2022), it would be crucial to install dedicated continuous multi-level samplers to understand the vertical salinity variability and the amount and the direction of saline groundwater seepage (de Louw et al., 2010). Finally, as described by Hermans et al. (2022), understanding the complex 4D interaction of factors, such as changes in groundwater extraction methods and land use, is crucial to get a more detailed comprehension of the salinization dynamics. Addressing these limitations is essential to develop effective management strategies to reduce its salinization impacts. Overall, the methodology adopted in this study has contributed to strengthen the hydrogeological conceptual model for the coastal area of Venice. This would not have been possible using conventional methods with short time series, providing many insights but also highlighting gaps in knowledge and suggesting necessary improvements for the monitoring network. However, the results of this study could be improved in the future when longer time series will be available.

4. Conclusions

In this paper, a systematic analysis of the time series in the time and frequency domains was proposed to improve the understanding of the hydrodynamic of a coastal shallow aquifer in the northern Adriatic coastal plain, at the southern margin of the Venice lagoon (Italy). The study area is an important and complex spot for agriculture and economic activities on a low-lying coast, which is built on a very fragile equilibrium between seawater intrusion and mechanical drainage. The heavy control and pressure exerted by human activities on the groundwater flow add on top of the already complex boundary conditions of the coastal aquifer, blurring the signals of the natural driving forces. Water level fluctuations in the Venice lagoon, driven by both natural forces (i.e. astronomic tides) and human uses (i.e. MoSE activation), represent the main upgradient Dirichlet condition that controls the variation of groundwater heads over most of the time, although isolated flooding/runoff events coming from the river-canal system overtake the signal during “wet periods”. In addition, the local effects of reclamation canals, tile-drains, and pumping cycles of the stations further complicate the picture and play an important role in the transient local variations of groundwater flow. The systematic time-series analysis described in the manuscript allowed the isolation of phenomena occurring at different time scales and frequencies, enabling a detailed investigation of each driver in the region. In addition, to tackle the main driving forces of the groundwater flow where they manifest, the analysis moves between different spatial scales, going from a regional meso-scale to address tides and precipitation, to a local site-specific scale to investigate the effect of canals, withdrawals, and tile-drains. It is worth remembering that the work was mainly based on scattered and irregular water-level datasets, established for different purposes, which usually miss an overall consistency to address the complexity of the flow and the seawater intrusion dynamics in the shallow aquifer. However, the rigorous process-centred approach, along with the numerical robustness of the MATLAB routine U_TIDE helped in addressing the challenges of a sparse data series and allowed identifying periodic tidal influences on all signals, from the Venice lagoon to the rivers, the canal, and the aquifer. The percentage of signal reconstructed using periodic harmonics (i.e. astronomic tides) resulted to be very significant in most of the high-frequency signals. Even if the signal percentages described by astronomical tidal constituents is almost halved in both piezometers focusing on the original signals, the tidal influence remains not negligible in comparison to the other aperiodic forcings and should not be overlooked when analysing groundwater dynamics in coastal areas. While EC signals were not well related to the

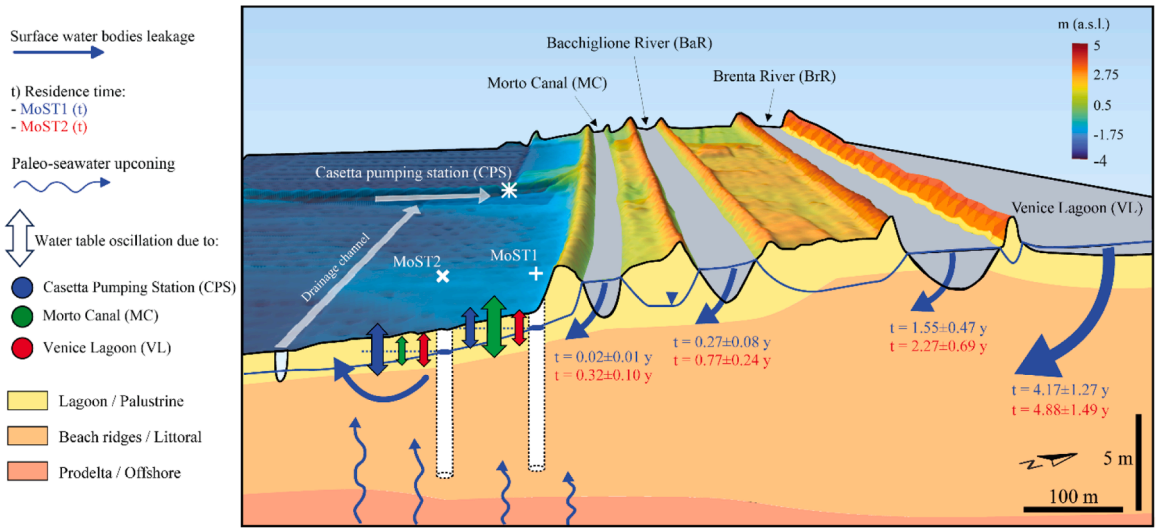

Fig. 12. 3D schematic representation of the hydrodynamic drivers in the Venice coastal aquifer, together with hydrogeological settings of depositional units. The digital elevation model with spatial resolution 5 m (DEM5) was retrieved from the LiDAR survey made by the Venice Lagoon Council of Basin.

aforementioned drivers, since the complex vertical salinity stratification in the aquifer combined with the screen length of the monitoring wells produced intra-borehole mixing that masked the aquifer salinization processes. Overall, the general approach of the work highlighted how to make use of sparse and incomplete time series to deepen the comprehension of a coastal shallow aquifer, while the specific findings cast light on the hydrodynamic governing the aquifer and help identifying flaws and uncertainties coming from the setup of the monitoring network in the area. Rising awareness of these weaknesses is the first and most important step to be able to improve current monitoring networks in this kind of fragile environment towards a 4D hydrogeology Hermans et al. (2022), addressing the current knowledge gaps and developing effective management strategies to ensure the sustainability of water resources.

CRediT authorship contribution statement

Marta Cosma: Writing – review & editing, Visualization. **Micòl Mastrocicco:** Writing – review & editing, Validation. **Luigi Tosi:** Writing – review & editing, Validation, Data curation, Conceptualization. **Sandra Donnici:** Writing – review & editing, Validation. **Fabrizio Rama:** Writing – review & editing, Supervision, Software, Methodology, Investigation, Formal analysis, Data curation, Conceptualization. **Mattia Gaiolini:** Writing – original draft, Visualization, Software, Methodology, Investigation, Formal analysis, Data curation, Conceptualization. **Nicolò Colombani:** Writing – review & editing, Validation, Supervision, Conceptualization.

Declaration of Competing Interest

The authors declare that they have no known competing financial interests or personal relationships that could have appeared to influence the work reported in this paper.

Acknowledgments

This research was supported by the EU co-financing the Interreg Italy–Croatia CBC Programme 2021–2027 (Cluster 2, Specific Objective 2.1) through the European Regional Development Fund as a part of the project “Subsurface WAter monitoring and Management to prevent drought risk in coastal systems” (SWAMrisk ID: ITHR0200479). The authors also acknowledge the project “Monitoring seawater intrusion in coastal aquifers and testing pilot projects for its mitigation” (MoST AID: 10047743).

Appendix A. Supporting information

Supplementary data associated with this article can be found in the online version at doi:10.1016/j.ejrh.2024.102039.

Data availability

Data will be made available on request.

References

Alessandrino, L., Gaiolini, M., Cellone, F.A., Colombani, N., Mastrocicco, M., Cosma, M., Da Lio, C., Tosi, L., 2023. Salinity origin in the coastal aquifer of the Southern Venice lowland. Sci. Total Environ. 905, 167058. https://doi.org/10.1016/j.scitotenv.2023.167058.

Amanambu, A.C., Obarein, O.A., Mossa, J., Li, L., Ayeni, S.S., Balogun, O., Oyebamiji, A., Ochege, F.U., 2020. Groundwater system and climate change: present status and future considerations. J. Hydrol. 589, 125163. https://doi.org/10.1016/j.jhydrol.2020.125163.

Baggio, G., Qadir, M., Smakhtin, V., 2021. Freshwater availability status across countries for human and ecosystem needs. Sci. Total Environ. 792, 148230. https://doi.org/10.1016/j.scitotenv.2021.148230.

Balugani, E., Antonellini, M., 2011. Barometric pressure influence on water table fluctuations in coastal aquifers of partially enclosed seas: an example from the Adriatic coast, Italy. J. Hydrol. 400 (1-2), 176–186. https://doi.org/10.1016/j.jhydrol.2011.01.040.

Bondesan, A., Furlanetto, P., 2012. Artificial fluvial diversions in the mainland of the lagoon of Venice during the 16th and 17th centuries inferred by historical cartography analysis. Geomorphologie (2), 175–200. https://doi.org/10.4000/geomorphologie.9815.

Brown, J.M., Bolaños, R., Howarth, M.J., Souza, A.J., 2012. Extracting sea level residual in tidally dominated estuarine environments. Ocean Dynam 62, 969–982. https://doi.org/10.1007/s10236-012-0543-.

Burri, N.M., Weatherl, R., Moeck, C., Schirmer, M., 2019. A review of threats to groundwater quality in the anthropocene. Sci. Total Environ. 684, 136–154. https://doi.org/10.1016/j.scitotenv.2019.05.236.

Carbognin, L., Gambolati, G., Putti, M., Rizzetto, F., Teatini, P., Tosi, L., 2006. Soil contamination and land subsidence raise concern in the Venice watershed, Italy. WIT Trans. Ecol. Envir. 99, 691–700. https://doi.org/10.2495/RAV060671.

Carbognin, L., Tosi, L., 2002. Interaction between climate changes, eustacy and land subsidence in the North Adriatic Region, Italy. Mar. Ecol. 23, 38–50. https://doi.org/10.1111/j.1439-0485.2002.tb00006.x.

Cavallina, C., Bergamasco, A., Cosma, M., Da Lio, C., Donnici, S., Tang, C., Tosi, L., Zaggia, L., 2022. Morpho-sedimentary constraints in the groundwater dynamics of low-lying coastal area: the Southern margin of the Venice Lagoon, Italy. Water 14 (17), 2717. https://doi.org/10.3390/w14172717.

Codiga, D.L., 2011. Unified tidal analysis and prediction using the UTide MATLAB functions. Technical report 2011-01. Graduate School of Oceanography, University of Rhode Island, Narragansett, RI, p. 59. https://doi.org/10.13140/RG.2.1.3761.2008.

Da Lio, C., Carol, E., Kruse, E., Teatini, P., Tosi, L., 2015. Saltwater contamination in the managed low-lying farmland of the Venice coast, Italy: an assessment of vulnerability. Sci. Total Environ. 533, 356–369. https://doi.org/10.1016/j. scitotenv.2015.07.013.

De Franco, R., Biella, G., Tosi, L., Teatini, P., Lozej, A., Chiozzotto, B., Giada, M., Rizzetto, F., Claude, C., Mayer, A., Bassan, V., Gasparetto-Stori, G., 2009. Monitoring the saltwater intrusion by time lapse electrical resistivity tomography: the Chioggia test site (Venice Lagoon, Italy). J. Appl. Geophys. 69 (3–4), 117–130. https://doi.org/10.1016/j.jappgeo.2009.08.004.

De Louw, P.G.B., Ouede Essink, G.H.P., Stuyfzand, P.J., Van der Zee, S.E.A.T.M., 2010. Upward groundwater flow in boils as the dominant mechanism of salinization in deep polders, The Netherlands. J. Hydrol. 394 (3–4), 494–506. https://doi.org/10.1016/j.jhydrol.2010.10.009.

De Marsily, G., 1986. Quantitative hydrogeology; Groundwater hydrology for engineers. Academic Press, p. 440. ISBN 10: 0122089162.

Delsman, J.R., 2015. Saline groundwater-Surface water interaction in coastal lowlands. IOS Press, Amsterdam the Netherlands, p. 188. https://doi.org/10.3233/978-1-61499-518-0-i.

Donnici, S., Serandrei-Barbero, R., Canali, G., 2012. Evidence of climatic changes in the Venetian Coastal Plain (Northern Italy) during the last 40,000 years. Sediment. Geol. 281, 139–150. https://doi.org/10.1016/j.sedgeo.2012.09.003.

Donnici, S., Serandrei-Barbero, R., Bini, C., Bonardi, M., Lezziero, A., 2011. The caranto paleosol and its role in the early urbanization of Venice. Geoarchaeology 26, 514–543. https://doi.org/10.1002/gea.20361.

Emery, W.J., Thomson, R.E., 2004. Data analysis methods in physical oceanography: third edition. Estuaries. https://doi.org/10.2307/1353059.

Enemark, T., Peeters, L.J., Mallants, D., Batelaan, O., 2019. Hydrogeological conceptual model building and testing: a review. J. Hydrol. 569, 310–329. https://doi.org/10.1016/j.jhydrol.2018.12.007.

Erol, S., 2011. Time-frequency analyses of tide-gauge sensor data. Sensors 11 (4), 3939–3961. https://doi.org/10.3390/s110403939.

Foster, S., Chilton, J., Nijsten, G.J., Richts, A., 2013. Groundwater—a global focus on the 'local resource. Curr. Opin. Env. Sust. 5 (6), 685–695. https://doi.org/10.1016/j.cosust.2013.10.010.

Foster, S., Garduño, H., 2013. Irrigated agriculture and groundwater resources–towards an integrated vision and sustainable relationship. Water Sci. Technol. 67 (6), 1165–1172. https://doi.org/10.2166/wst.2013.654.

Frascaroli, F., Parrinello, G., Root-Bernstein, M., 2021. Linking contemporary river restoration to economics, technology, politics, and society: perspectives from a historical case study of the Po River Basin, Italy. Ambio 50 (2), 492–504. https://doi.org/10.1007/s13280-020-01363-3.

Gattacceca, J.C., Vallet-Coulomb, C., Mayer, A., Claude, C., Radakovitch, O., Conchetto, E., Hamelin, B., 2009. Isotopic and geochemical characterization of salinization in the shallow aquifers of a reclaimed subsiding zone: the southern Venice Lagoon coastland. J. Hydrol. 378 (1–2), 46–61. https://doi.org/10.1016/j.jhydrol.2009.09.005.

Ghezzo, M., Guerzoni, S., Cucco, A., Umgiesser, G., 2010. Changes in Venice Lagoon dynamics due to construction of mobile barriers. Coast. Eng. 57 (7), 694–708. https://doi.org/10.1016/j.coastaleng.2010.02.009.

Green, T.R., Taniguchi, M., Kooi, H., Gurdak, J.J., Allen, D.M., Hiscock, K.M., Treidel, H., Aureli, A., 2011. Beneath the surface of global change: impacts of climate change on groundwater. J. Hydrol. 405 (3–4), 532–560. https://doi.org/10.1016/j.jhydrol.2011.05.002.

Han, D., Currell, M.J., Cao, G., Hall, B., 2017. Alterations to groundwater recharge due to anthropogenic landscape change. J. Hydrol. 554, 545–557. https://doi.org/10.1016/j.jhydrol.2017.09.018.

Heiss, J.W., Michael, H.A., 2014. Saltwater-freshwater mixing dynamics in a sandy beach aquifer over tidal, spring-neap, and seasonal cycles. Water Resour. Res. 50, 6747–6766. https://doi.org/10.1002/2014WR015574.

Hermans, T., Goderniaux, P., Jougnot, D., Fleckenstein, J., Brunner, P., Nguyen, F., Linde, N., Huisman, J.N., Bour, O., Alvis, J.L., Hoffmann, R., Palacios, A., Cooke, A. K., Pardo-Alvarez, A., Blazevic, L., Pouladi, B., Haruzi, P., Fernandez Visentini, A., Nogueira, G.E.H., Tirado-Conde, J., Looms, M.C., Kenshilikova, M., Davy, P., Le Borgne, T., 2022. Advancing measurements and representations of subsurface heterogeneity and dynamic processes: towards 4D hydrogeology. Hydrol. Earth Syst. Sci. Discuss. 27 (1), 255–287. https://doi.org/10.5194/hess-27-255-2023.

Hilhorst, M.A., 2000. A pore water conductivity sensor. Soil Sci. Soc. Am. J. 64 (6), 1922–1925. https://doi.org/10.2136/sssaj2000.6461922x.

Khorrami, M., Malekmohammadi, B., 2021. Effects of excessive water extraction on groundwater ecosystem services: vulnerability assessments using biophysical approaches. Sci. Total Environ. 799, 149304. https://doi.org/10.1016/j.scitotenv.2021.149304.

Labat, D., 2005. Recent advances in wavelet analyses: Part 1. A review of concepts. J. Hydrol. 314 (1-4), 275–288. https://doi.org/10.1016/j.jhydrol.2005.04.003.

Lovrinović, I., Bergamasco, A., Srzić, V., Cavallina, C., Holjević, D., Donnici, S., Erceg, J., Zaggia, L., Tosi, L., 2021. Groundwater monitoring systems to understand sea water intrusion dynamics in the Mediterranean: the Neretva valley and the Southern Venice coastal aquifers case studies. Water 13 (4), 561. https://doi.org/10.3390/w13040561.

Lovrinović, I., Srzić, V., Aljinović, I., 2023. Characterization of seawater intrusion dynamics under the influence of hydro-meteorological conditions, tidal oscillations and melioration system operative regimes to groundwater in Neretva valley coastal aquifer system. J. Hydrol. 46, 101363. https://doi.org/10.1016/j.ejrh.2023.101363.

Luo, X., Kwok, K.L., Liu, Y., Jiao, J., 2017. A permanent multilevel monitoring and sampling system in the coastal groundwater mixing zones. Groundwater 55 (4), 577–587. https://doi.org/10.1111/gwat.12510.

Malki, M., Bouchaou, L., Hirich, A., Brahim, Y.A., Choukr-Allah, R., 2017. Impact of agricultural practices on groundwater quality in intensive irrigated area of Chtouka-Massa, Morocco. Sci. Total Environ. 574, 760–770. https://doi.org/10.1016/j.scitotenv.2016.09.145.

Mao, X., Enot, P., Barry, D.A., Li, L., Binley, A., Jeng, D.S., 2006. Tidal influence on behaviour of a coastal aquifer adjacent to a low-relief estuary. J. Hydrol. 327 (1-2), 110–127. https://doi.org/10.1016/j.jhydrol.2005.11.030.

Mastrocicco, M., Colombani, N., 2021. The issue of groundwater salinization in coastal areas of the mediterranean region: a review. Water 13 (1), 90. https://doi.org/10.3390/w13010090.
Mastrocicco, M., Giambastiani, B.M.S., Severi, P., Colombani, N., 2012. The importance of data acquisition techniques in saltwater intrusion monitoring. Water Resour. Manag. 26, 2851–2866. https://doi.org/10.1007/s11269-012-0052-y.
MathWorks Inc, 2023. MATLAB version: 9.13.0 (R2023b). The MathWorks Inc, Natick, Massachusetts. ⟨https://www.mathworks.com⟩.
Matte, P., Jay, D.A., Zaron, E.D., 2013. Adaptation of classical tidal harmonic analysis to nonstationary tides, with application to river tides. J. Atmos. Ocean. Tech. 30 (3), 569–589. https://doi.org/10.1175/JTECH-D-12-00016.1.
Naganna, S.R., Deka, P.C., Ch, S., Hansen, W.F., 2017. Factors influencing streambed hydraulic conductivity and their implications on stream–aquifer interaction: a conceptual review. Environ. Sci. Pollut. R. 24, 24765–24789. https://doi.org/10.1007/s11356-017-0393-4.
Nevill, J.C., Hancock, P.J., Murray, B.R., Ponder, W.F., Humphreys, W.F., Phillips, M.L., Groom, P.K., 2010. Groundwater-dependent ecosystems and the dangers of groundwater overdraft: a review and an Australian perspective. Pac. Conserv. Biol. 16 (3), 187–208. https://doi.org/10.1071/PC100187.
Parrinello, G., Bizzi, S., Surian, N., 2021. The retreat of the delta: a geomorphological history of the Po River basin during the twentieth century. Water Hist. 13 (1), 117–136. https://doi.org/10.1007/s12685-021-00279-3.
Pawlowicz, R., Beardsley, B., Lentz, S., 2002. Classical tidal harmonic analysis including error estimates in MATLAB using T_TIDE. Comput. Geosci. 28 (8), 929–937. https://doi.org/10.1016/S0098-3004(02)00013-4.
Pousa, J., Tosi, L., Kruse, E., Guaraglia, D., Bonardi, M., Mazzoldi, A., Rizzetto, F., Schnack, E., 2007. Coastal processes and environmental hazards: the Buenos Aires (Argentina) and Venetian (Italy) littorals. Environ. Geol. 51, 1307–1316. https://doi.org/10.1007/s00254-006-0424-9.
Pugh, D.T., 1987. Tides, surges and mean sea level. Wiley, Swindon, UK. ⟨http://eprints.soton.ac.uk/id/eprint/19157⟩.
Rama, F., Miotlinski, K., Franco, D., Corseuil, H.X., 2018. Recharge estimation from discrete water-table datasets in a coastal shallow aquifer in a humid subtropical climate. Hydrogeol. J. 26 (6), 1887–1902. https://doi.org/10.1007/s10040-018-1742-1.
Rojas, R., Kahunde, S., Peeters, L., Batelaan, O., Feyen, L., Dassargues, A., 2010. Application of a multimodel approach to account for conceptual model and scenario uncertainties in groundwater modelling. J. Hydrol. 394 (3–4), 416–435. https://doi.org/10.1016/j.jhydrol.2010.09.016.
Saito, L., Christian, B., Diffley, J., Richter, H., Rohde, M.M., Morrison, S.A., 2021. Managing groundwater to ensure ecosystem function. Groundwater 59 (3), 322–333. https://doi.org/10.1111/gwat.13089.
Sánchez-Úbeda, J.P., Calvache, M.L., Duque, C., López-Chicano, M., 2016. Filtering methods in tidal-affected groundwater head measurements: application of harmonic analysis and continuous wavelet transform. Adv. Water Resour. 97, 52–72. https://doi.org/10.1016/j.advwatres.2016.08.016.
Schweizer, D., Ried, V., Rau, G.C., Tuck, J.E., Stoica, P., 2021. Comparing methods and defining practical requirements for extracting harmonic tidal components from groundwater level measurements. Math. Geosci. 53, 1147–1169. https://doi.org/10.1007/s11004-020-09915-9.
Shalev, E., Lazar, A., Wollman, S., Kington, S., Yechieli, Y., Gvirtzman, H., 2009. Biased monitoring of fresh water-salt water mixing zone in coastal aquifers. Groundwater 47 (1), 49–56. https://doi.org/10.1111/j.1745-6584.2008.00502.x.
Shi, L., Jiao, J.J., 2014. Seawater intrusion and coastal aquifer management in China: a review. Environ. Earth Sci. 72, 2811–2819. https://doi.org/10.1007/s12665-014-3186-9.
Storms, J.E.A., Weltje, G.J., Terra, G.J., Cattaneo, A., Trincardi, F., 2008. Coastal dynamics under conditions of rapid sea-level rise: late Pleistocene to Early Holocene evolution of barrier–lagoon systems on the northern Adriatic shelf (Italy). Quat. Sci. Rev. 27, 1107–1123. https://doi.org/10.1016/j.quascirev.2008.02.009.
Straffelini, E., Tarolli, P., 2023. Climate change-induced aridity is affecting agriculture in Northeast Italy. Agric. Syst. 208, 103647. https://doi.org/10.1016/j.agsy.2023.103647.
Teatini, P., Tosi, L., Strozzi, T., Carbognin, L., Wegmüller, U., Rizzetto, F., 2005. Mapping regional land displacements in the Venice coastland by an integrated monitoring system. Remote Sens. Environ. 98 (4), 403–413. https://doi.org/10.1016/j.rse.2005.08.002.
Torresan, S., Critto, A., Rizzi, J., Marcomini, A., 2012. Assessment of coastal vulnerability to climate change hazards at the regional scale: the case study of the North Adriatic Sea. Nat. Hazards Earth Syst. Sci. 12, 2347–2368. https://doi.org/10.5194/nhess-12-2347-2012.
Tosi, L., Carbognin, L., Teatini, P., Rosselli, R., Gasparetto Stori, G., 2000. In: Carbognin, L., Gambolati, G., Johnson, A.I. (Eds.), The ISES Project subsidence monitoring of the catchment basin south of the Venice Lagoon (Italy). Land Subsidence, vol. II, C.N.R. - Gruppo nazionale per la difesa dalle catastrofi idrogeologiche, Perugia, pp. 113–126. ISBN 88-87222-06-1.
Tosi, L., Da Lio, C., Bergamasco, A., Cosma, M., Cavallina, C., Fasson, A., Viezzoli, A., Zaggia, L., Donnici, S., 2022. Sensitivity, hazard, and vulnerability of farmlands to saltwater intrusion in low-lying coastal areas of Venice, Italy. Water 14 (1), 64. https://doi.org/10.3390/w14010064.
Tosi, L., Da Lio, C., Strozzi, T., Teatini, P., 2016. Combining L- and X-Band SAR interferometry to assess ground displacements in heterogeneous coastal environments: the Po River Delta and Venice Lagoon, Italy. Remote Sens 8 (4), 308. https://doi.org/10.3390/rs8040308.
Tosi, L., Rizzetto, F., Zecchin, M., Brancolini, G., Baradello, L., 2009a. Morphostratigraphic framework of the Venice Lagoon (Italy) by very shallow water VHRS surveys: evidence of radical changes triggered by human-induced river diversions. Geophys. Res. Lett. 36. https://doi.org/10.1029/2008GL037136.
Tosi, L., Teatini, P., Carbognin, L., Brancolini, G., 2009b. Using high resolution data to reveal depth-dependent mechanisms that drive land subsidence: the venice coast, Italy. Tectonophysics 474 (1–2), 271–284. https://doi.org/10.1016/j.tecto.2009.02.026.
Umgiesser, G., 2020. The impact of operating the mobile barriers in Venice (MOSE) under climate change. J. Nat. Conserv. 54, 125783. https://doi.org/10.1016/j.jnc.2019.125783.
Viezzoli, A., Tosi, L., Teatini, P., Silvestri, S., 2010. Surface water–groundwater exchange in transitional coastal environments by airborne electromagnetics: the Venice Lagoon example. Geophys. Res. Lett. 37. https://doi.org/10.1029/2009GL041572.
Zecchin, M., Brancolini, G., Tosi, L., Rizzetto, F., Caffau, M., Baradello, L., 2009. Anatomy of the Holocene succession of the southern Venice lagoon revealed by very high-resolution seismic data. Cont. Shelf Res. 29, 1343–1359. https://doi.org/10.1016/j.csr.2009.03.006.
Zhang, H., 2021. Characterization of a multi-layer karst aquifer through analysis of tidal fluctuation. J. Hydrol. 601, 126677. https://doi.org/10.1016/j.jhydrol.2021.126677.